

Stacked Intelligent Metasurface-Aided Wave-Domain Signal Processing: From Communications to Sensing and Computing

Jiancheng An, *Senior Member, IEEE*, Chau Yuen, *Fellow, IEEE*, Marco Di Renzo, *Fellow, IEEE*, Mehdi Bennis, *Fellow, IEEE*, and Mérouane Debbah, *Fellow, IEEE*, and Lajos Hanzo, *Life Fellow, IEEE*

arXiv:2601.16030v1 [cs.IT] 22 Jan 2026

Abstract—Neural networks possess incredible capabilities for extracting abstract features from data. Electromagnetic computing harnesses wave propagation to execute computational operations. Metasurfaces, composed of subwavelength meta-atoms, are capable of engineering electromagnetic waves in unprecedented ways. What happens when combining these three cutting-edge technologies? This question has sparked a surge of interest in designing physical neural networks using stacked intelligent metasurface (SIM) technology, with the aim of implementing various computational tasks by directly processing electromagnetic waves. SIMs open up an exciting avenue toward high-speed, massively parallel, and low-power signal processing in the electromagnetic domain. This article provides a comprehensive overview of SIM technology, commencing with its evolutionary development. We subsequently examine its theoretical foundations and existing SIM prototypes in depth. Furthermore, the optimization/training strategies conceived to configure SIMs for achieving the desired functionalities are discussed from two different perspectives. Additionally, we explore the diverse applications of SIM technology across the communication, sensing, and computing domains, presenting experimental evidence that highlights its distinctive advantages in supporting multiple functions within a single device. Finally, we identify critical technical challenges that must be addressed to deploy SIMs in next-generation wireless networks and shed light on promising research directions to unlock their full potential.

I. INTRODUCTION

THE past decade has witnessed tremendous advances in artificial intelligence (AI) [1]. In particular, multi-layer artificial neural networks (ANNs), inspired by the architecture of biological neural networks in the human brain, have demonstrated exceptional capabilities in a wide range of applications, such as computer vision [2], speech recognition [3], and natural language processing [4]. An ANN is composed of artificial neurons that are typically aggregated into layers,

J. An and C. Yuen are with the School of Electrical and Electronics Engineering, Nanyang Technological University (NTU), Singapore 639798 (e-mail: jiancheng_an@163.com, chau.yuen@ntu.edu.sg).

M. Di Renzo is with Université Paris-Saclay, CNRS, CentraleSupélec, Laboratoire des Signaux et Systèmes, 3 Rue Joliot-Curie, 91192 Gif-sur-Yvette, France, and with King's College London, Department of Engineering - Centre for Telecommunications Research, WC2R 2LS London, United Kingdom (e-mail: marco.di_renzo@kcl.ac.uk).

M. Bennis is with the Centre for Wireless Communications, University of Oulu, 90570 Oulu, Finland (e-mail: mehdi.bennis@oulu.fi).

M. Debbah is with Khalifa University of Science and Technology, P O Box 127788, Abu Dhabi, UAE (e-mail: merouane.debbah@ku.ac.ae).

L. Hanzo is with the School of Electronics and Computer Science, University of Southampton, Southampton SO17 1BJ, U.K. (e-mail: lh@ecs.soton.ac.uk).

with connections to other neurons in adjacent layers through synaptic edges. Each artificial neuron processes the signals it receives from connected neurons and sends a signal to the downstream neurons [5]. By training the connection weights of each edge in a data-driven manner, ANNs acquire the ability to learn abstract features of the input data, enabling them to handle complex tasks.

Analog electromagnetic computing (or wave-domain computing) has also gained considerable attention in recent years due to its ability to efficiently tackle complex mathematical operations, such as spatial integration, differentiation, and convolution, as well as solving equations by leveraging the propagation of waves within custom-designed material slabs or cavities [6]. Electromagnetic computing has been found to significantly enhance the information processing efficiency compared to conventional computing paradigms, thanks to its unique characteristics of light-speed operation, low energy consumption, and scalability for massively parallel processing [7]. Recent research studies have showcased the substantial potential of electromagnetic computing in various practical scenarios [6], particularly in high-volume real-time data processing scenarios, such as augmented reality and autonomous driving.

Additionally, the rapidly advancing field of engineered metamaterials has led to the emergence of programmable metasurfaces and information metasurfaces [8], [9]. A metasurface is essentially an artificial planar surface composed of periodically arranged subwavelength scattering meta-atoms [10], [11]. By tuning external stimuli, such as mechanical deformation or bias voltage using field programmable gate arrays (FPGA), each individual meta-atom can independently modulate the phase and/or amplitude of incident electromagnetic waves [12], [13]. This breakthrough technology has opened up new possibilities for manipulating electromagnetic wavefronts at an unprecedented scale to achieve a wide range of functionalities, spanning from planar hologram generation to the customization of communication environments [14].

The fusion of neural network architectures with electromagnetic computing has catalyzed the development of diffractive neural networks (DNNs) [15]. As illustrated in Fig. 1, a DNN is implemented using a number of densely packed diffractive layers, with free-space propagation between them. In a dielectric diffractive layer, the thickness of each individual pixel (or neuron) is a learnable variable that can be adjusted to control the transmission coefficient [15]. After adequate training and

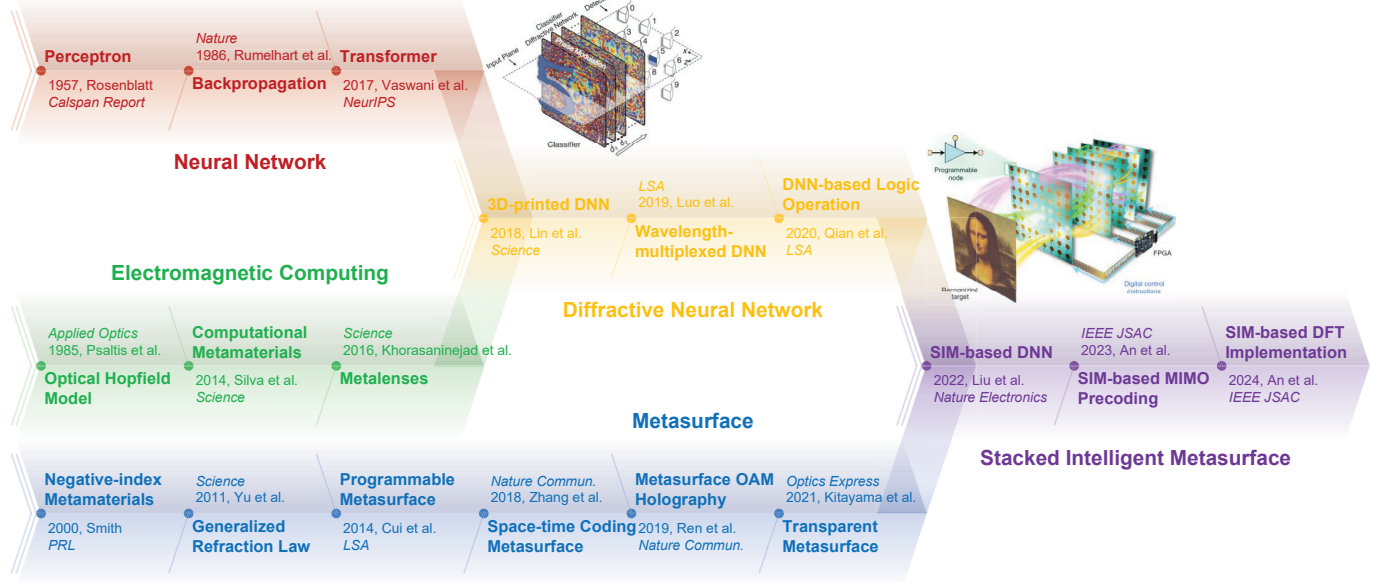


Fig. 1: The evolution timeline of the SIM technology.

fabrication using three-dimensional (3D) printing techniques, a DNN can carry out specific functions through the interactions of electromagnetic waves within the diffractive layers. Various advanced DNN architectures have been reported in the recent literature, demonstrating impressive capabilities in many emerging applications, including image classification and reconstruction [16], real-time object detection [17], and matrix inversion [18].

However, DNNs constructed with passive diffractive layers have a significant limitation: once they are fabricated, they cannot be retrained to perform other tasks. This restriction severely hinders their potential for widespread deployment. Fortunately, the emergence of programmable metasurfaces provides the missing piece of the puzzle to create reconfigurable DNNs [19]. As shown in Fig. 1, by stacking several intelligent metasurfaces into a single device, a new technology is conceived, which is referred to as a stacked intelligent metasurface (SIM) [20], [21]. In a SIM, each intelligent metasurface functions as a layer of a DNN, and each programmable meta-atom is analogous to a neuron with learnable phase and amplitude responses, which can be adjusted to accommodate the requirements of diverse tasks in dynamic environments. Consequently, a SIM inherits the powerful representation capabilities of ANNs, the ultra-fast speed of electromagnetic computing, as well as the energy-efficient electromagnetic tuning capability of programmable metasurfaces [21].

SIMs represent a revolutionary and transformative technology that has the potential to fundamentally reshape the future of communication, sensing, and computing. In this article, we provide a comprehensive overview of SIM technology, examining its vast potential and the fundamental challenges in its practical applications. Specifically, our contributions are summarized below:

- 1) We commence by elucidating the fundamental SIM

principles, encompassing its physical architecture and neural network counterparts. We further present a comprehensive review of advances in SIM prototype development. The configuration (or training, in DNN jargon) strategies for SIM are also examined from two different perspectives.

- 2) We critically appraise the applications of SIM in communication, sensing, and computing systems, presenting experimental findings that demonstrate the distinctive advantages of SIM technology. Additionally, the promising potential for integrating communication, sensing, and computing functionalities within a unified SIM framework is discussed to enable emerging applications.
- 3) We shed light on both the substantial opportunities and critical challenges inherent in translating the innovative SIM concept into a practical technology, addressing considerations in modeling, protocol design, and potential energy efficiency concerns. Furthermore, we provide insights into pathways for enhancing both the signal processing and inference capabilities of SIMs.

To outline our exploration of SIM technology, the structure of this article is illustrated in Fig. 2.

II. ELECTROMAGNETIC FOUNDATION OF SIM

From a physical perspective, a SIM is constructed by stacking multiple layers of reconfigurable transmissive metasurfaces. According to the Huygens–Fresnel principle [19], each meta-atom on a metasurface layer functions as a secondary source, producing a spherical wave that illuminates all the meta-atoms on the next layer. The phase and amplitude of the diffracted secondary wave that impinges on the next layer are jointly determined by the electromagnetic waves impinging upon the meta-atoms on the current layer, by the complex-valued transmission coefficients of the current layer,

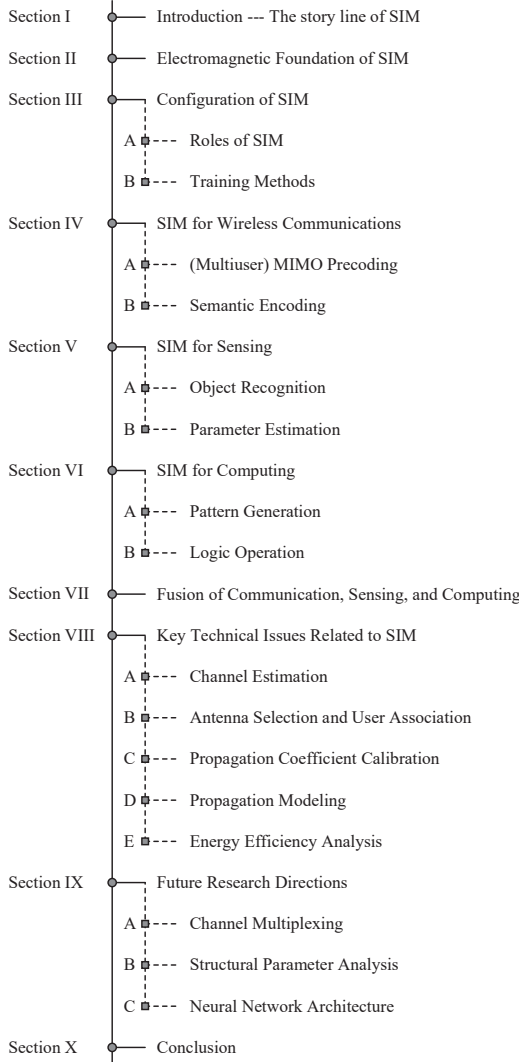


Fig. 2: The organization of this paper.

and by the complex-valued propagation coefficients (in free space) between the two layers considered [21], [22]. Based on the Rayleigh–Sommerfeld diffraction integral [15], [23], the propagation coefficient between the \tilde{n} -th meta-atom on the $(l-1)$ -st metasurface layer and the n -th meta-atom on the l -th metasurface layer is given by¹

$$w_{n,\tilde{n}}^l = \frac{\mathcal{A} \cos \zeta_{n,\tilde{n}}^l}{d_{n,\tilde{n}}^l} \left(\frac{1}{2\pi d_{n,\tilde{n}}^l} - j \frac{1}{\lambda} \right) e^{j2\pi d_{n,\tilde{n}}^l/\lambda}, \quad (1)$$

where $d_{n,\tilde{n}}^l$ denotes the corresponding transmission distance. Furthermore, \mathcal{A} is the area of each meta-atom, $\zeta_{n,\tilde{n}}^l$ represents the angle between the propagation direction and the normal direction of the $(l-1)$ -st metasurface layer, and λ represents the radio wavelength. The total electromagnetic field that

¹The propagation model in (1) allows us to account for near-field propagation between adjacent metasurface layers, but it can be applied provided that some physical conditions are fulfilled. Notably, the (sub-wavelength) inter-layer distance cannot be too small, so as to ensure that (1) is physically consistent. As a rule of thumb, the inter-layer distance, given the size of meta-atoms, should be sufficiently large to ensure that the amplitude of (1) is less than one [24].

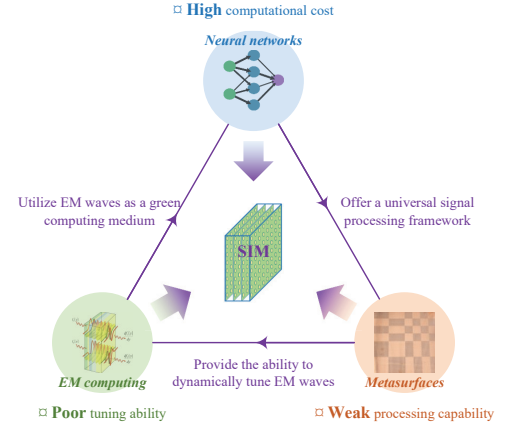


Fig. 3: SIM is the amalgamation of neural networks, electromagnetic computing, and metasurfaces. The advantages of these three technologies complement each other.

impinges upon each meta-atom on a metasurface layer is the sum of the fields refracted by all the meta-atoms on the previous layer [20].

The architecture of a SIM is similar to that of an ANN. Explicitly, both consist of an input layer, one or more hidden layers, and an output layer [19], [25]. In a SIM, each hidden layer is essentially a metasurface, which is a dense array of electronically programmable meta-atoms that function similarly to artificial neurons in a conventional digital ANN. The meta-atoms on different layers are interconnected through the diffraction of electromagnetic waves. In principle, each meta-atom in a SIM can potentially impact any other meta-atom. However, in practical SIM devices, anti-reflective coatings can be utilized to suppress unwanted back-and-forth reflections and limit the electromagnetic coupling between non-adjacent layers [17]. As a result, a SIM is equivalent to a feed-forward diffraction device, where electromagnetic waves propagate from one layer to the next. In contrast to conventional ANNs, the complex-valued connection weights, or propagation coefficients, between metasurface layers in a SIM are not individually trainable [15]. Instead, they are explicitly dictated by the propagation direction and the axial spacing between layers. The trainable network parameters in a SIM-based DNN are the transmission coefficients of the meta-atoms at specific lattice coordinates [18].

A SIM fundamentally represents a synergistic integration of three interdisciplinary technologies: neural networks, electromagnetic computing, and information metasurfaces [14]. As illustrated in Fig. 3, these three cutting-edge technologies exhibit complementary strengths that address each other's inherent limitations. Conventional neural networks, while powerful, depend on digital chips that incur substantial computational overhead and energy consumption [5]. Metasurfaces, despite their sophisticated wavefront manipulation capabilities, possess limited signal processing functionality [8]. Similarly, existing electromagnetic computing paradigms suffer from constrained tunability and poor scalability [6]. A SIM circumvents these limitations by synthesizing the distinct advantages

TABLE I: A survey of existing SIM prototypes.

# Reference b Author h Year	Prototype	◊ SIM architecture ♣ Per-layer size ♡ Inter-layer spacing ♠ Phase modulation	⊗ Task ⊖ Loss function ◎ Dataset	f: Frequency λ: Wavelength	Output	Performance
# [15] b Lin <i>et al.</i> h 2018		◊ 200 × 200 × 5 ♣ 8 cm × 8 cm ♡ 3 cm ♠ [0, π)	⊗ Image classification ⊖ Energy distribution ◎ MNIST	f: 0.40 THz λ: 0.75 mm	10 detection regions	Classification accuracy 91.75% (Simulation) 80.74% (Experiment)
		◊ 300 × 300 × 5 ♣ 9 cm × 9 cm ♡ 4 cm ♠ [0, 2π)	⊗ Image classification ⊖ Energy distribution ◎ Fashion-MNIST			Classification accuracy 81.13% (Simulation) 73.02% (Experiment)
		◊ 30 × 42 × 2 ♣ 30 cm × 42 cm ♡ 30 cm ♠ [0, 2π)	⊗ Amplitude imaging ⊖ MSE ◎ ImageNet	Plane: 9 cm × 9 cm		Resolution 1.2 mm (Simulation) 1.8 mm (Experiment)
# [26] b Qian <i>et al.</i> h 2020		◊ 30 × 42 × 2 ♣ 30 cm × 42 cm ♡ 30 cm ♠ [0, 2π)	⊗ Logic operation ⊖ MSE ◎ ---	f: 17 GHz λ: 1.76 mm	2 detection regions	Contrast ratio > 9.6 dB
# [16] b Li <i>et al.</i> h 2021		◊ 160 × 160 × 3 ♣ 8 cm × 8 cm ♡ 3 cm ♠ 12 bits	⊗ Image classification ⊖ Softmax CE error ◎ MNIST	f: 0.21 THz ~ 0.30 THz λ: 1.00 mm ~ 1.45 mm	1 broadband detector with 10 wavelengths	Classification accuracy 96.01%
			⊗ Image classification ⊖ Softmax CE error ◎ EMNIST	f: 0.19 THz ~ 0.46 THz λ: 0.65 mm ~ 1.60 mm	1 broadband detector with 20 wavelengths	Classification accuracy 96.04%
			⊗ Image classification ⊖ Softmax CE error ◎ EMNIST	f: 0.21 THz ~ 0.36 THz λ: 0.83 mm ~ 1.45 mm	1 broadband detector with 26 wavelengths	Classification accuracy 84.05%
			⊗ Multi-beam focusing ⊖ MSE ◎ ---	f: 0.20 THz ~ 0.40 THz λ: 0.76 mm ~ 1.52 mm	1 broadband detector with 52 wavelengths	Classification accuracy 85.60%
# [19] b Liu <i>et al.</i> h 2022		◊ 8 × 8 × 5 ♣ 56 cm × 56 cm ♡ 10 cm ♠ 4 bits	⊗ Image classification ⊖ CE error ◎ 'I' and '[]'	f: 5.40 GHz λ: 5.56 cm	2 detection regions	Classification accuracy 100%
			⊗ Image classification ⊖ CE error ◎ MNIST		10 detection regions	Classification accuracy 90.76%
			⊗ CDMA ⊖ MSE ◎ ---	f: 5.50 GHz λ: 5.45 cm	4 detection regions	Bit error rate 5.2×10^{-3}
			⊗ Multi-beam focusing ⊖ MSE ◎ ---		2 target points	Energy leakage < 10%
# [27] b Gu <i>et al.</i> h 2023		◊ 32 × 32 × 3 ♣ 34 cm × 34 cm ♡ 18 cm ♠ [0, 2π)	⊗ Image classification ⊖ CE error ◎ MNIST	f: 11 GHz λ: 2.73 cm	10 detection regions	Classification accuracy 90%
# [28] b Wang <i>et al.</i> h 2024		◊ 16 × 16 × (1 ~ 3) ♣ 31 cm × 31 cm ♡ 1.29 cm ~ 10.34 cm ♠ 1 bit	⊗ Signal enhancement ⊖ Received power ◎ ---	f: 5.80 GHz λ: 5.17 cm	1 receiving antenna	Power gain 7 dB
# [29] b Gao <i>et al.</i> h 2024		◊ 32 × 32 × 3 ♣ 27.45 cm × 27.45 cm ♡ 5.45 cm ♠ 7 bits	⊗ DOA estimation ⊖ MSE & CE error ◎ ---	f: 25 GHz ~ 30 GHz λ: 1.0 cm ~ 1.2 cm	10 detection regions	Angular resolution 3° in [-15°, 15°]
		◊ 32 × 32 × 4 ♣ 27.45 cm × 27.45 cm ♡ 5.45 cm ♠ 7 bits				Angular resolution 1° in [-5°, 5°]
# [30] b Guo <i>et al.</i> h 2025		◊ 100 × 100 × 2 ♣ 2.5 cm × 2.5 cm ♡ 1 cm ♠ [0, 2π)	⊗ Image classification ⊖ MSE ◎ EMNIST	f: 0.60 THz λ: 0.50 mm	4 detection regions	Classification accuracy 92.50%

of all three constituent technologies. Specifically, electromagnetic waves serve as a ‘green’ - namely power-efficient - computational medium for executing forward-propagation inference in neural networks, while neural network architectures provide a versatile framework for signal processing. Concurrently, information metasurfaces enable dynamic modulation

of electromagnetic waves, completing this potent tripartite amalgam.

Once the programmable metasurfaces are properly configured, the SIM becomes capable of processing spatial electromagnetic waves as they propagate through the layered structure [31]. Since a SIM directly processes information-

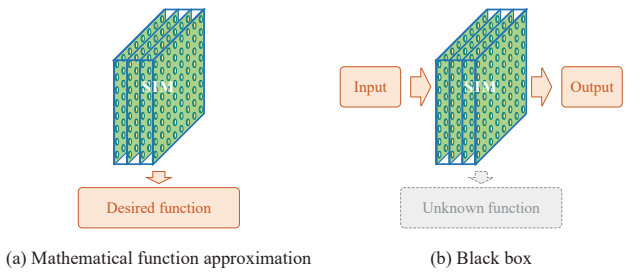


Fig. 4: Two SIM configuration methods depending on whether the desired transfer function is known or not.

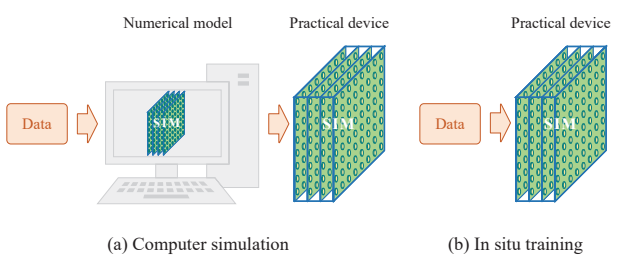


Fig. 5: Two SIM configuration methods depending on whether there is an accurate numerical model or not.

carrying electromagnetic waves in free space, it can execute desired computation tasks without requiring any digital storage, transmission, pre-processing of information, as well as external computing power [14]. Most remarkably, information processing within a SIM takes place at the speed of light [20]. Additionally, a SIM can be readily scaled up to accommodate extremely large-scale inputs and a plethora of connections in a cost-effective and power-efficient manner [19]. Thanks to these distinctive advantages, several advanced SIMs have been designed to carry out various tasks in the wave domain [15], [16], [19], [26]–[29]. For a more detailed overview, Table I provides a comprehensive review of existing SIM prototypes, including their functions and corresponding hardware parameters, to guide practical SIM designs.

III. CONFIGURATION OF SIMS

As previously mentioned, designing a well-configured SIM is crucial for it to perform the intended functions and complete a given inference task [14]. In this section, we elaborate on potential strategies conceived for optimizing and training the transmission coefficients of SIMs from two different perspectives.

A. Roles of a SIM

As shown in Fig. 4, one can distinguish two primary roles for a SIM according to whether the transformation desired is known or unknown.

- **Mathematical Function Approximation:** In certain application scenarios, the desired transformation matrix – such as the discrete Fourier transform (DFT) used in spectral analysis – is known in advance [31]. In these

cases, a SIM can be employed to approximate the desired function by tuning the transmission coefficients of multiple metasurface layers. While a digital signal processor can achieve the same function, the utilization of a SIM allows one to achieve near-instantaneous computing, thanks to its electromagnetic-domain signal processing [20]. In general, the approximation of desired functions imposes lower requirements on reconfigurability. Therefore, the SIM may only have to be reconfigured on a relatively long timescale [14], [31].

- **Black Box:** In most practical applications, however, such as image classification, the target transformation is often unknown [17]. In these scenarios, a SIM can be optimized as a “black box.” By feeding it with a large number of training samples, the complex-valued transmission coefficients within the SIM can be iteratively adjusted based on their gradients with respect to a custom-designed loss function tailored to the specific task [16]. Since SIMs are physically assembled subject to diverse fabrication constraints imposed on phase and amplitude modulation, the transmission coefficients have to be quantized to feasible values that can be practically implemented by individual meta-atoms [19].

B. Training Methods

From the perspective of the training process, the transmission coefficients can be trained using either computer simulations or directly on a physical SIM device, as indicated in Fig. 5.

- **Computer Simulation:** Similar to an ANN, the training of a SIM can be executed on a computer. Once the transmission coefficients are trained to achieve a satisfactory level of approximation accuracy or inference performance, they are deployed on the SIM [15]. Although the training time is constrained by the processing power of the digital computer, the forward propagation during the inference stage occurs at the speed of light. However, computer simulations also pose significant challenges, as they require a reliable mathematical model or simulation tool that can instantly and accurately quantify the complex interactions of wave propagation within the SIM. While established numerical methods, such as the finite-difference time-domain (FDTD) method and finite-elements method (FEM), offer high accuracy, there is still potential for improving their simulation speed [29].
- **In Situ Training:** In practice, hardware implementations of metasurfaces may diverge from their numerical models due to deformations that occur during the manufacturing process and undesired misalignments between layers. This may lead to inaccurate inference outcomes. To address this issue, an alternative approach known as in situ training has shown considerable potential [32], [33]. Since the training and inference processes share the same electromagnetic responses, any fabrication imperfections and mechanical misalignments are implicitly accounted for during the training phase, resulting in minimal impact on the inference results. Additionally, the training time is

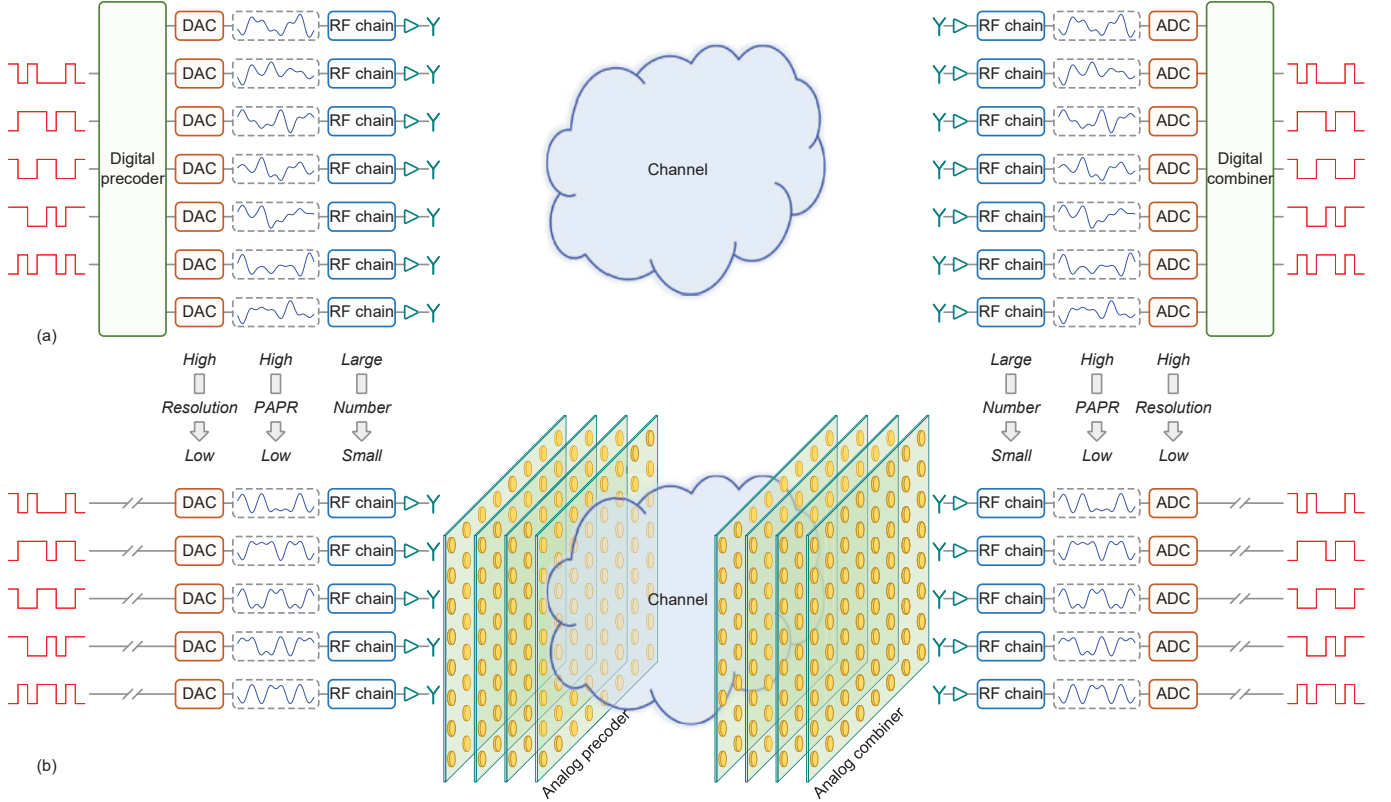


Fig. 6: A comparison between (a) conventional MIMO architecture and (b) SIM-based MIMO architecture.

substantially reduced, because the forward propagation of signals occurs at the speed of light [19]. Moreover, in situ training enables the application of deep reinforcement learning (DRL) strategies [34], which can train the transmission coefficients based on practical observations in a dynamic environment. However, in situ training needs real-time feedback from the output, which introduces extra signaling overhead when the SIM is deployed far from the inference receiver [20].

Once appropriately configured, SIMs can be utilized to perform a variety of inference tasks by directly processing information carried by electromagnetic waves. To elaborate on the unique capabilities of SIMs, we next provide a critical appraisal of its potential applications in communication (Sec. IV), sensing (Sec. V), and computing (Sec. VI) systems.

IV. SIMS FOR WIRELESS COMMUNICATIONS

In wireless communication systems, modulation, filtering, and beamforming are particularly crucial for effectively conveying information, for shaping desired signal waveforms, and for directing beams toward intended users [35]. As a promising alternative to traditional baseband processing techniques, SIMs can accomplish these tasks more efficiently in the wave domain.

A. MIMO Precoding

In the pioneering work [20], a pair of SIMs was employed at the transmitter and receiver for automatically implementing

multiple-input multiple-output (MIMO) precoding and combining, as the electromagnetic waves propagate through the well-configured metasurfaces. With the use of SIMs, MIMO transceivers can eliminate the need for complex matrix multiplications in the digital domain. This substantially reduces processing latency, hardware costs, and energy usage compared to conventional MIMO systems [20]. Furthermore, the hardware complexity can be reduced by transforming complex multi-stream detection schemes into parallel single-stream detection schemes. Building on this concept, the authors of [36], [37] applied the SIM-based transceiver design concept to multiuser multiple-input single-output (MISO) downlink communications. In this scenario, a SIM was integrated with the radome of the base station (BS) to carry out transmit beamforming directly in the electromagnetic wave domain. To maximize the sum rate of all users, an optimization problem was formulated by jointly optimizing transmit power allocation and analog beamforming in the wave domain, subject to constraints on the transmit power budget and phase shifts. By decomposing the joint optimization problem into two sub-problems, the power allocation sub-problem was addressed using the popular iterative water-filling algorithm, while the SIM was configured through successive refinement for discrete phase shift tuning [37] and gradient ascent (GA) for continuous phase shift tuning [36].

To illustrate the associated conceptual differences, Fig. 6 contrasts a conventional MIMO system with a SIM-based MIMO system. In conventional MIMO communication systems, multiple data streams are superimposed by a digital

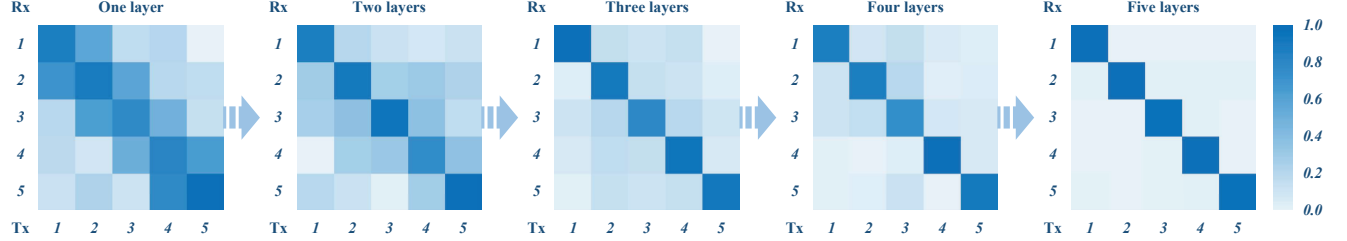


Fig. 7: Example of a 5×5 MIMO channel, where a pair of SIMs are employed and optimized to perform precoding and combining in the wave domain. Therefore, the five data streams can be transmitted and received in parallel through the corresponding antennas, without interfering with each other.

TABLE II: A comparison of SIM-based MIMO systems with their conventional counterparts in terms of computational complexity and hardware architecture.

Scenario	# of sub-carriers	# of UEs	# of BSs	SIM	Reference	Year	# of RF chains	Complexity order
MIMO	$N_{\text{SC}} = 1$	$N_{\text{UE}} = 1$	$N_{\text{BS}} = 1$	✗	Goldsmith <i>et al.</i> [38]	2003	$N_{\text{RF}} = N_{\text{Tx}}$	$\mathcal{O}(N_{\text{Tx}}N_{\text{Stream}})$
				✓	An <i>et al.</i> [20]	2023	$N_{\text{RF}} = N_{\text{Stream}}$	$\mathcal{O}(1)$
Multiuser	$N_{\text{SC}} = 1$	$N_{\text{UE}} > 1$	$N_{\text{BS}} = 1$	✗	Spencer <i>et al.</i> [39]	2004	$N_{\text{RF}} = N_{\text{Tx}}$	$\mathcal{O}(N_{\text{Tx}}N_{\text{UE}})$
				✓	An <i>et al.</i> [37]	2024	$N_{\text{RF}} = N_{\text{UE}}$	$\mathcal{O}(1)$
Cell-free	$N_{\text{SC}} = 1$	$N_{\text{UE}} > 1$	$N_{\text{BS}} > 1$	✗	Ngo <i>et al.</i> [40]	2017	$N_{\text{RF}} = N_{\text{BS}}N_{\text{Tx}}$	$\mathcal{O}(N_{\text{BS}}N_{\text{Tx}}N_{\text{UE}})$
				✓	Shi <i>et al.</i> [41]	2024	$N_{\text{RF}} \leq N_{\text{BS}}N_{\text{UE}}$	$\mathcal{O}(1)$
OFDM	$N_{\text{SC}} > 1$	$N_{\text{UE}} = 1$	$N_{\text{BS}} = 1$	✗	Bolcskei <i>et al.</i> [42]	2002	$N_{\text{RF}} = N_{\text{Tx}}$	$\mathcal{O}(N_{\text{Tx}}N_{\text{Stream}} + N_{\text{Tx}} \log N_{\text{SC}})$
				✓	Li <i>et al.</i> [43]	2024	$N_{\text{RF}} = N_{\text{Stream}}$	$\mathcal{O}(N_{\text{Stream}} \log N_{\text{SC}})$

◇ N_{Tx} : Number of transmit antennas at each BS; ◇ N_{Stream} : Number of data streams.

precoder at the baseband before transmission [35]. However, this process produces signals having high peak-to-average power ratios (PAPR), which, in turn, necessitate high-resolution digital-to-analog converters (DACs) and analog-to-digital converters (ADCs) for accurate processing. Moreover, the resultant high PAPR reduces the efficiency of power amplifiers (PA) at the transmitter and low-noise amplifiers (LNA) at the receiver [14]. By contrast, SIM-based MIMO systems perform transmit precoding and receive combining in the wave domain, thereby eliminating the need for digital precoding and combining [20]. As a consequence, each antenna only transmits a single data stream. When employing low-order modulation schemes, low-resolution DACs and ADCs become adequate, since the modulated waveforms typically exhibit low PAPRs. In addition, the number of radio-frequency (RF) chains in SIM-based systems is reduced to match the number of data streams (or users), leading to significant reductions in both hardware cost and energy consumption [21], [22].

Additionally, Fig. 7 illustrates the actions of an end-to-end MIMO channel utilizing the SIM-based architecture of Fig. 6(b). A pair of SIMs is employed to mitigate interference among five data streams. The system operates at 28 GHz. Moreover, each metasurface consists of 10×10 meta-atoms arranged with half-wavelength spacing. The axial spacing between adjacent metasurface layers is set to one wavelength, while all other simulation parameters are consistent with those outlined in [21]. The transmission coefficients of the transmitting and receiving SIMs are optimized using the gradient descent (GD) method described in [20]. As seen from Fig. 7, by utilizing an adequate number of metasurface layers, it

becomes possible to create multiple interference-free channels, even in the absence of digital precoding and combining.

Over the past few years, the concept of utilizing SIMs to implement precoding in the wave domain has gained considerable attention and has been applied to various communication systems [60]. Next, we will review the notable progress in this area from three key perspectives.

- **From Far-Field Communications to Near-Field Communications:** In order to simultaneously achieve high data throughput and massive connectivity in next-generation wireless networks, extremely large-scale antenna arrays (ELAAs) and metasurfaces are expected to be widely deployed [61]. As a consequence, wireless communications will predominantly operate in the radiating near-field region. Although the fundamental system design and signal processing techniques for near-field and far-field communications are similar, the unique characteristics of spherical wavefronts in near-field propagation offer enhanced spatial multiplexing gain [61], [62]. Furthermore, in addition to angular selectivity, they also allow ‘spot-light-like’ beam-focusing to a specific location, hence allowing for the distinction of users in the distance domain. However, this advantage necessitates complex matrix operations for baseband beamfocusing at the transmitter, which can lead to high computational complexity and processing delays when using ELAAs or metasurfaces. In this context, applying a SIM to perform near-field beamfocusing in the wave domain becomes increasingly appealing. Building on this idea, Jia *et al.* [63] explored the potential of SIMs in multiuser MISO near-

TABLE III: A survey of existing studies on SIM, with a focus on optimization problem formulation and solver.

Ref.	Link	Optimization problem	Solution	Characteristic	⊗ Variables & ⊙ Constraints
[44]	—	$\min \sum_{s=1}^S \sum_{\tilde{s} \neq s} h_{s,\tilde{s}} ^2$ ⊗ {v ₁ } ⊙ {C ₁ }	Layer-by-layer optimization, closed-form solution	Two SIMs	* SIM v ₁ : ψ _n ^l , ∀n, ∀l v ₂ : ψ _n ^l [t], ∀n, ∀l, ∀t v ₃ : ζ _n ^l , ∀n, ∀l
[45]	—	$\max C$ ⊗ {v ₁ , v ₆ } ⊙ {C ₁ , C ₈ , C ₉ }	Projected GA	Two SIMs	
[46]	—	$\max R_C$ ⊗ {v ₁ , v ₆ } ⊙ {C ₁ , C ₈ , C ₉ }	Projected GA	Two SIMs, discrete alphabet	
[47]	DL	$\max \sum_{k=1}^K R_k$ ⊗ {v ₁ , v ₄ } ⊙ {C ₁ , C ₄ , C ₆ }	DDPG	n.a.	
[48]	DL		TD3	n.a.	
[49]	DL		<u>AO</u> {v ₁ : Projected GA v ₄ : Weighted MMSE}	Statistical CSI	○ RIS v ₇ : θ _m , ∀m v ₈ : ρ _m , ∀m
[50]	DL	$\max \sum_{k=1}^K R_k$ ⊗ {v ₁ , v ₃ , v ₄ } ⊙ {C ₁ , C ₃ , C ₄ , C ₆ }	<u>AO</u> {v ₁ , v ₃ : Projected GA v ₄ : Iterative WF}	Active layers, user scheduling	◇ UAV v ₉ : q _k [t], ∀k, ∀t
[51]	DL	$\max \sum_{k=1}^K R_k$	TD3, meta-learning	Passive RIS, user mobility	* SIM C ₁ : ψ _n ^l ∈ [0, 2π), ∀n, ∀l C ₂ : ψ _n ^l [t] ∈ [0, 2π), ∀n, ∀l, ∀t C ₃ : ζ _n ^l ≤ ζ _{max} , ∀n, ∀l
[52]	DL	⊗ {v ₁ , v ₄ , v ₇ } ⊙ {C ₁ , C ₄ , C ₆ , C ₁₀ , C ₁₄ }	NAC, meta-learning	STAR-RIS, user mobility	
[53]	DL	$\max \left(\prod_{k=1}^K R_k \right)^{1/K}$ ⊗ {v ₁ , v ₄ } ⊙ {C ₁ , C ₄ , C ₆ }	Consensus ADMM	Rate fairness	* Transmitter C ₄ : $\sum_{s=1}^S p_s \leq P_{\max}$ C ₅ : $\sum_{k=1}^K p_k[t] \leq P_{\max}, \forall t$ C ₆ : p _s ≥ 0, ∀s C ₇ : p _k [t] ≥ 0, ∀k, ∀t C ₈ : tr(Q) ≤ P _{max} C ₉ : Q ⊇ 0
[54]	DL	$\max \sum_{k=1}^K O_k$ ⊗ {v ₁ , v ₄ } ⊙ {C ₁ , C ₄ , C ₆ , C ₁₆ }	CQL, meta-learning	QoE, user mobility	
[55]	DL	$\max N_{\text{UE}}$ ⊗ {v ₁ , v ₄ , v ₈ } ⊙ {C ₁ , C ₄ , C ₆ , C ₁₀ , C ₁₁ , C ₁₄ }	MPO, meta-learning	Active RIS, user mobility	
[56]	UL	$\max \sum_{k=1}^K R_k$ ⊗ {v ₁ } ⊙ {C ₁ }	Projected GA	Ambient SIM	○ RIS C ₁₀ : θ _m ∈ [0, 2π), ∀m C ₁₁ : ρ _m ≤ ρ _{max} , ∀m
[57]	DL	$\max \sum_{t=1}^T \sum_{k=1}^K R_k[t]$	D4PG, meta-learning	UAV, user mobility	◇ UAV C ₁₂ : q _k [t+1] - q _k [t] ≤ v _{max} τ, ∀k, ∀t C ₁₃ : q _k [t] ∈ Q, ∀k, ∀t
[58]	DL	⊗ {v ₂ , v ₅ , v ₉ } ⊙ {C ₂ , C ₅ , C ₇ , C ₁₂ , C ₁₃ , C ₁₅ }	<u>AO</u> {v ₂ : GA v ₅ : FP v ₉ : DQN}	Digital twin, flight control	● QoS / QoE C ₁₄ : R _k ≥ R _{min} , ∀k C ₁₅ : R _k [t] ≥ R _{min} , ∀t C ₁₆ : O _k ≥ O _{min} , ∀k
[59]	DL	$\min \ x - \hat{x}\ ^2$ ⊗ {v ₁ } ⊙ {C ₁ }	Layer-by-layer optimization, closed-form solution	PLS, reduced power loss	

field communications, where a SIM was integrated into the radome of a BS to perform beamfocusing through wave manipulation. They employed a GD algorithm to configure the transmission coefficients of a SIM and customize an end-to-end channel that minimizes interference among users. Moreover, the authors of [64] formulated an optimization problem aimed at maximizing the weighted sum rate of multiple near-field users by jointly designing the transmit power allocation and the phase shifts of the

SIM. A block coordinate descent (BCD) algorithm was then applied to solve this problem.

- **From Narrowband Beamforming to Wideband Beamforming:** Traditional wideband MIMO communication systems deal with different frequency bands separately through digital beamforming [65]. By contrast, a SIM has to process multiple frequency sub-bands using a single device, which can lead to the deleterious beam squint phenomenon [66] – where the beam direction varies

TABLE IV: The major symbols in Table III and their meanings.

Symbol	Meaning	Symbol	Meaning
$p_k[t]$	Transmit power allocated to the k -th user at time slot t	v_{\max}	Maximum flight velocity
$\psi_n^l[t]$	Phase shift of the n -th meta-atom on the l -th metasurface layer at time slot t	τ	Duration of each time slot
$\mathbf{q}_k[t]$	Position of the k -th user at time slot t	\mathcal{Q}	Air corridor
$R_k[t]$	Achievable rate of the k -th user at time slot t	T	Number of time slots
ϱ_m	Amplitude of the m -th RIS element	ϱ_{\max}	Maximum amplitude provided by the active load
ς_n^l	Amplitude response of the n -th meta-atom on the l -th metasurface layer	s_{\max}	Maximum amplitude response
p_k	Power allocated to the k -th user	P_{\max}	Maximum transmit power
O_k	Mean opinion score of the web service for user k	O_{\min}	Minimum QoE level
R_k	Achievable rate of the k -th user	R_{\min}	QoS requirement
p_s	Power allocated to the s -th data stream	K	Number of users
ψ_n^l	Phase shift of the n -th meta-atom on the l -th metasurface layer	θ_m	Phase shift of the m -th RIS element
\mathbf{Q}	Transmit covariance matrix	N_{UE}	Number of served users
$h_{s,\tilde{s}}$	End-to-end channel from the \tilde{s} -th transmit antenna to the s -th receive antenna	S	Number of data streams
\mathbf{x}	The actual signal output by the last layer of the SIM	R_C	Channel cutoff rate
$\hat{\mathbf{x}}$	The desired signal output by the last layer of the SIM	C	Channel capacity

with frequency. However, unlike single-layer metasurfaces that maintain a frequency-flat profile, SIMs can produce frequency-selective transfer functions thanks to their multiple internal propagation paths. Inspired by this characteristic, Li *et al.* [43] explored the application of SIMs for fully-analog beamforming in MIMO-aided orthogonal frequency division multiplexing (OFDM) communication systems, which aims to achieve interference-free transmission across a broad frequency range. To achieve this, they employed a GD algorithm to determine the optimal SIM configuration and examined the relationship between the maximum effective transmission bandwidth and various physical parameters of the SIM, such as the number of metasurface layers and the metasurface aperture. Their numerical results demonstrated that optimizing the SIM for multiple frequency sub-carriers – rather than only the center frequency – significantly improved the channel capacity of SIM-aided MIMO-OFDM communication systems. Furthermore, in [67], the same authors adopted index modulation (IM)-aided OFDM as the transmission waveform to illuminate SIM. In OFDM-IM, information is conveyed by selectively activating a subset of available subcarriers, with the specific indices of these active subcarriers implicitly conveying additional bits. This transmission strategy offers two key advantages: firstly, the selective subcarrier activation inherently reduces the PAPR of the broadband transmission waveform; secondly, the sparse subcarrier multiplexing among multiple users effectively expands the operational bandwidth over which a SIM can function effectively. To assess system reliability, the worst-case bit error rate (BER) was adopted as the performance metric, and a deep unfolding framework was developed for configuring the SIM parameters, while adaptively adjusting the step size at each iteration.

- **From Single BS to Multiple BSs:** The capacity of wireless networks can be enhanced by deploying more BSs or access points (APs); however, this approach also increases both the hardware costs and energy consump-

tion accordingly [68]. To tackle this challenge, recent studies have investigated the integration of low-cost SIMs with APs in cell-free massive MIMO systems. In downlink scenarios, Hu *et al.* [69] developed a method that jointly optimizes AP power allocation and SIM-based wave-domain beamforming to maximize the sum rate. For uplink applications, Shi *et al.* [41], [70] developed a two-stage transmission framework. The first stage employs a greedy algorithm to minimize interference among pilot signals during channel estimation. In the second stage, the SIM is configured to achieve wave-domain beamforming, and a power allocation algorithm is developed for maximizing the worst-case spectral efficiency of user equipment (UE). Additionally, Li *et al.* [71] optimized the SIM coefficients for accurately recovering the symbols for each UE. The central processing unit (CPU) then combined the local detection results using weights designed based on the minimum mean square error (MMSE) criteria, taking into account the impact of hardware impairments. These studies demonstrate that increasing the number of metasurface layers can significantly reduce inter-user interference by effectively leveraging wave manipulation. More recently, Park *et al.* [72] proposed a hybrid beamforming approach that combines wave-domain beamforming through SIMs with standard digital processing. Specifically, an optimization framework was developed for jointly configuring the digital beamforming, wave-domain beamforming, and fronthaul compression for maximizing the weighted sum-rate of both the uplink and downlink, when fronthaul capacity is limited.

To further illustrate the benefits of SIM-based MIMO systems, Table II compares the number of RF chains required and the computational complexity involved in implementing beamforming in these communication systems versus their conventional counterparts. As shown in Table II, the utilization of SIM not only facilitates efficient beamforming in the wave domain but also significantly reduces both the hardware costs and computation demands. Moreover, recent research has

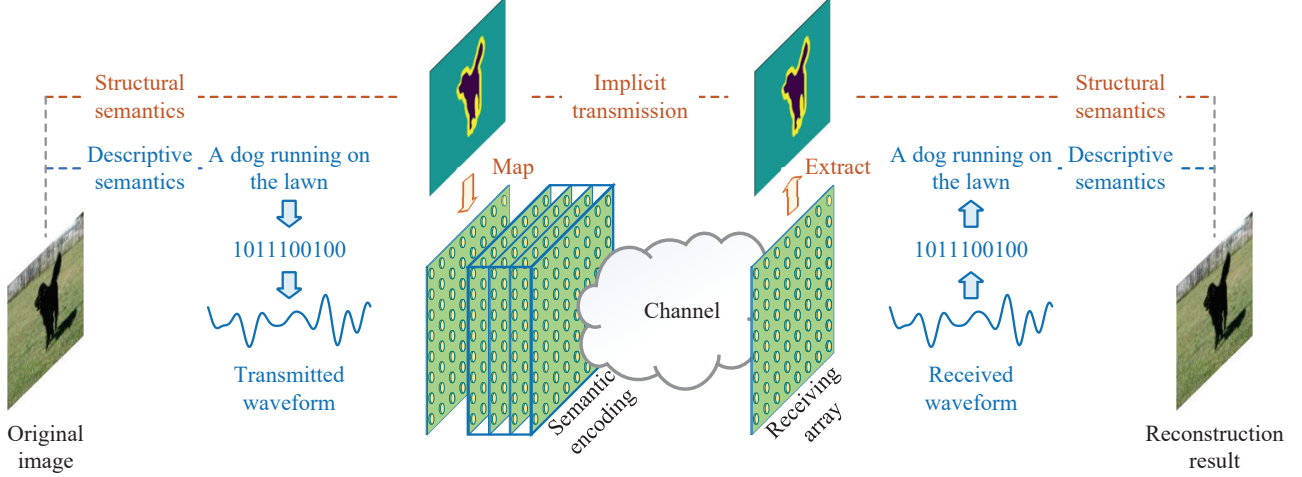


Fig. 8: An application of SIMs in bimodal semantic communication systems, where the structural semantic information is implicitly conveyed by imaging the edge patterns onto the receiving array, while the descriptive semantic information is transmitted using traditional phase-amplitude modulation techniques. The receiver subsequently reconstructs the original image by synthesizing the received bimodal semantic information.

also explored the integration of SIM with other emerging wireless technologies, such as DRL [47], [48], [51], [73]–[75], reconfigurable intelligent surfaces (RIS) [52], [55], [56], rate splitting multiple access (RSMA) [76], [77], and unmanned aerial vehicles (UAV) [57], [58]. Other sophisticated applications include physical layer security (PLS) [59], [78], non-orthogonal multiple access (NOMA) [79], and simultaneous wireless information and power transfer (SWIPT) [80], by taking advantage of the capability of SIM to efficiently process signals in the wave domain. To provide a comprehensive understanding of these recent advances from a mathematical perspective, Table III summarizes typical optimization problem formulations, including the popular optimization objectives, key optimization variables, constraints, as well as common solvers. Additionally, the relevant mathematical symbols and their definitions are listed in Table IV.

B. Semantic Encoding

Semantic communication is a promising paradigm that can significantly enhance communication efficiency. In task-oriented semantic communication systems, a SIM can be utilized as a semantic encoder. For example, the authors of [81] demonstrated this concept by investigating a classification task in which a SIM was strategically positioned before the transmit antenna. The input layer of the SIM was utilized for source encoding, while the remaining layers formed a DNN for semantic encoding, which aims for transforming the signals traversing the input layer into a unique beam directed toward the receiving antenna corresponding to a specific class. In contrast to conventional communication systems that transmit modulated signals containing either encoded information or compressed semantic information, the transmit antenna of SIM-based semantic communication systems simply emits unmodulated electromagnetic carrier waves [81]. At the receiver, the image class is recognized by probing the signal magnitude distributions across the receiving array, which substantially

reduces the required signal processing complexity. Notably, both the source and semantic encoding occur automatically as the electromagnetic waves propagate through the stratified structure. By adopting a similar philosophy, Liu *et al.* [82] developed a disaster recognition method that consists of a SIM mounted on a drone to process semantic information encoded in electromagnetic waves, while dissipating low energy and at extremely fast speeds. At the ground station, the electronic network further processes the received signals to improve the system's ability to make more accurate disaster predictions.

When transmitting complex visual scenes, existing semantic communication systems encounter challenges related to substantial data transmission demands. To address this issue, Huang *et al.* [83] leveraged a SIM placed in front of the transmit antenna to convey visual edge information from intricate scenes by directly mapping them using imaging techniques onto the receiver array, as illustrated in Fig. 8. Complementary textual scene descriptions are transmitted using traditional amplitude and phase modulation techniques. To realize the desired function, a customized mini-batch GD algorithm was developed for fine-tuning the transmission coefficients of meta-atoms within the SIM, thereby minimizing discrepancies between the received and desired visual patterns. Subsequently, a conditional generative adversarial network (GAN) processes the received visual patterns and text descriptions to reconstruct the complex original scene.

V. SIM FOR SENSING

Wireless sensing is essential for acquiring critical information about targets of interest. Typical sensing applications encompass direction-of-arrival (DOA) estimation, object recognition, as well as target detection and tracking. In contrast to traditional sensing algorithms that rely on specific models and cannot meet real-time processing requirements, SIM provides a universal framework for extracting information by directly processing radio waves.

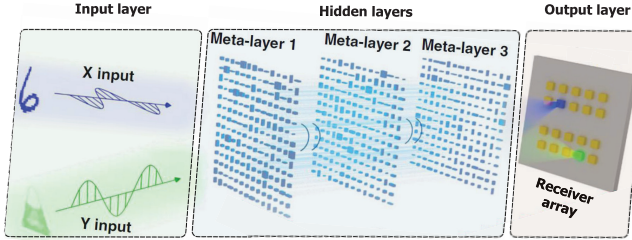


Fig. 9: A schematic diagram depicting the application of SIM to target recognition, with SIM operating as a physical neural network.

A. Object Recognition

Substantial research efforts have established that SIM has great potential in executing object recognition tasks [15], [19]. Building upon this foundation, Luo *et al.* [17] fabricated an advanced polarization-multiplexed SIM that operates in the visible spectrum, which demonstrates the capability to simultaneously perform dual recognition tasks: identifying handwritten digits and classifying fashionable items by using distinct polarization channels. As shown in Fig. 9, this innovative dual-channel object classification framework consists of three primary components:

- *Input layer*: A plane wave with appropriately engineered phase and amplitude distribution is used for encoding the object information across multiple channels.
- *Hidden layers*: Each hidden layer contains asymmetric meta-atoms with tunable birefringence characteristics.
- *Output layer*: The physical output plane is partitioned into several discrete detection regions, each corresponding to a particular object category.

By employing an error backpropagation approach, the multi-dimensional phase distributions are progressively updated, and, eventually, much of the energy of the input electromagnetic waves gleaned from different channels is correctly routed to their corresponding detection regions. The region having the highest intensity at the output layer indicates the class identified. Both computational simulations and experimental validation have confirmed that using a SIM with a deeper architecture can substantially enhance the recognition performance [17]. For instance, the accuracy of recognizing 10 handwritten digits improves from 65% to 92%, when increasing the number of metasurface layers from one to seven (as illustrated in Fig. 2(a) of [17]).

In addition to polarization multiplexing, a broadband SIM was developed in [16] to perform statistical inference by encoding the spatial features of objects into spectral power distributions at preselected wavelengths, with each representing a different classification category. The SIM is trained to maximize the power of the specific spectral component corresponding to the true label of each object. As a result, a single-pixel detector at the output plane becomes sufficient for analyzing the power distribution across the spectrum and for performing object classification. Additionally, a compact fully-connected ANN having merely two hidden layers was trained for successfully reconstructing the image of the input

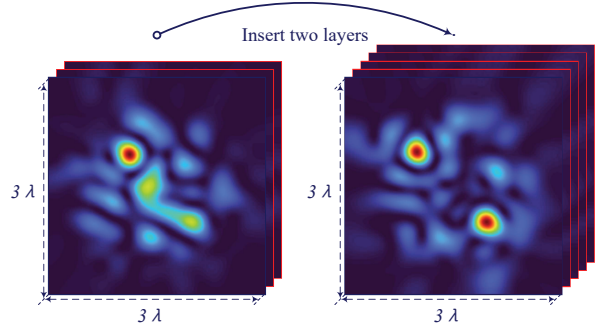


Fig. 10: Spatial frequency spectra produced by a two-layer and four-layer SIM, when two targets are present. The metasurface layers are spaced by one wavelength, each consisting of 10×10 half-wavelength spaced meta-atoms.

objects based on the highly compressed spectral power representations [16], even if they were misclassified by the SIM. Recently, Hua *et al.* [84] presented AirFC, a representative paradigm that leverages SIM to enable over-the-air computation for low-latency and energy-efficient analog inference with enhanced image classification accuracy.

B. Parameter Estimation

Wireless sensing relying on radio wave propagation constitutes a fundamental enabler for diverse applications spanning communication, radar, and navigation systems [85], [86]. Conventional paradigms for target detection and parameter estimation rely upon an intricate process that involves the RF front-end circuitry to demodulate and sample multi-channel baseband signals, followed by computationally intensive algorithmic operations that inherently impose stringent limitations on sensing latency and energy efficiency (EE) [87]. By contrast, a SIM offers a compelling alternative by directly processing electromagnetic waves to estimate target parameters, thereby bypassing the conventional requirements for RF circuitry, ADCs, and digital signal processing infrastructure.

Recent years have witnessed growing research interest in leveraging SIMs for DOA estimation [29], [88]–[90]. The fundamental mechanism underlying SIM-based DOA estimation lies in spatially mapping the electromagnetic field distributions impinging from different source directions into distinct angular bins. Typically, a SIM is positioned in front of a detector array, where each detection region corresponds to a specific angular interval and captures the intensity of the received electromagnetic field. Through optimization of the control voltages applied to individual meta-atoms, the SIM can be trained to focus the energy of the incident waves arriving from targets at particular angles onto their corresponding detection regions at the output plane. In [88], Huang *et al.* demonstrated the feasibility of SIM-based DOA estimation for multiple incident sources across wide frequency and angular ranges. By optimizing the physical parameters of the SIM, their sensing architecture creates distinct virtual channels that isolate and process different incoming wavefronts, enabling automatic beam classification and spatial routing based on incidence

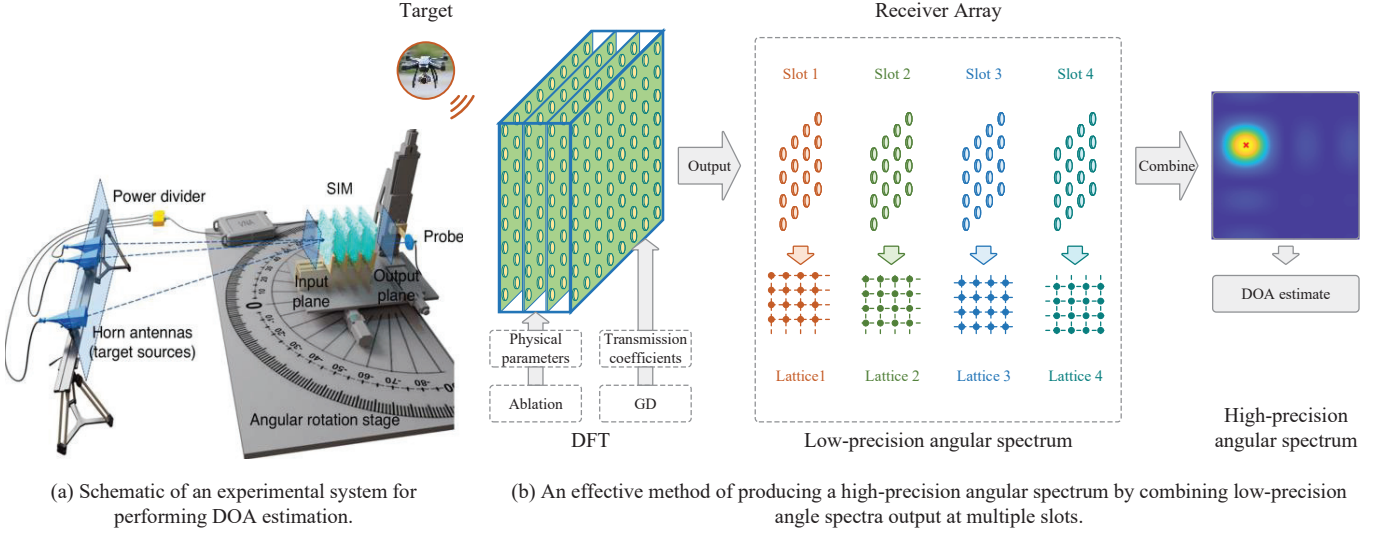


Fig. 11: Illustration of employing SIM for DOA estimation.

TABLE V: The experimental energy distribution matrix and confusion matrix are evaluated on the single-target testing data set, where target angle interval i represents the angular range of $[(i - 6)^\circ, (i - 5)^\circ]$.

	Energy distribution matrix										Confusion matrix									
	Angle interval										Angle interval									
	1	2	3	4	5	6	7	8	9	10	1	2	3	4	5	6	7	8	9	10
Probe 1	0.44	0.19	0.05	0.01	0.03	0.03	0.02	0.01	0.00	0.00	10	0	0	0	0	0	0	0	0	0
Probe 2	0.32	0.33	0.24	0.09	0.01	0.02	0.04	0.03	0.01	0.02	0	10	0	0	0	0	0	0	0	0
Probe 3	0.12	0.25	0.30	0.21	0.06	0.01	0.03	0.04	0.02	0.01	0	0	10	0	0	0	0	0	0	0
Probe 4	0.06	0.13	0.23	0.30	0.24	0.10	0.03	0.01	0.01	0.00	0	0	0	10	0	0	0	0	0	0
Probe 5	0.01	0.03	0.10	0.22	0.30	0.25	0.12	0.03	0.03	0.04	0	0	0	0	10	0	0	0	0	0
Probe 6	0.02	0.01	0.01	0.10	0.23	0.27	0.18	0.06	0.00	0.03	0	0	0	0	10	0	0	0	0	0
Probe 7	0.01	0.02	0.03	0.03	0.07	0.17	0.24	0.23	0.12	0.02	0	0	0	0	0	0	10	0	0	0
Probe 8	0.01	0.02	0.02	0.01	0.03	0.09	0.19	0.28	0.27	0.14	0	0	0	0	0	0	0	10	0	0
Probe 9	0.01	0.01	0.02	0.02	0.01	0.05	0.14	0.26	0.32	0.30	0	0	0	0	0	0	0	0	10	0
Probe 10	0.00	0.00	0.00	0.00	0.01	0.01	0.00	0.06	0.23	0.44	0	0	0	0	0	0	0	0	0	10

angle and frequency. Their experimental implementation employed a dual-layer SIM to detect multiple sources within the $8 \sim 12$ GHz frequency band for incident angles ranging from -30° to 30° . The results demonstrated significant reductions in both processing time and energy consumption compared to traditional DOA estimation techniques.

To experimentally validate the DOA estimation performance attained, Gao *et al.* [29] implemented a SIM operating at 27.5 GHz. As illustrated in Fig. 11(a), the experimental configuration utilized a vector network analyzer (VNA) connected to horn antennas serving as target sources and a waveguide probe for signal detection. The detection region of the waveguide probe was precisely controlled via a translation stage, while a four-layer passive SIM architecture was designed and fabricated to estimate azimuth angles with 1° angular resolution over the range $[-5^\circ, 5^\circ]$. Each metasurface layer consisted of a 32×32 array of modulation elements with half-wavelength spacing of 5.45 mm. The output plane was partitioned into ten distinct detection regions, each mapped to a specific input angular range. Experimental validation using 100 test samples yielded energy distributions and confusion matrices presented

in Tab. V, demonstrating that energy is concentrated at the probe corresponding to the angular interval of the incident wave. Through temporal multiplexing of different SIM configurations with varying angular resolutions and coverage ranges, this approach enables precise DOA estimation of multiple targets across an extended field of view [29].

Additionally, SIMs can function as electromagnetic signal processors, offering a compelling alternative to conventional digital computation. For instance, by finely tuning the transmission coefficients of all meta-atoms, a SIM can implement a two-dimensional (2D) DFT by strategically engineering wave propagation characteristics [31], [89]. This capability holds considerable promise for sensing applications having stringent requirements on computing latency. By applying an electromagnetic-domain DFT operator in front of a receiving array, incident electromagnetic waves automatically undergo transformation into the spatial frequency domain as they propagate through the optimized SIM structure [31]. Consequently, the target DOA can be directly determined by analyzing signal intensity distributions across the receiving array. To further enhance the DOA estimation accuracy, An *et al.* [31] aggregated

the spatial frequency spectra observed in multiple snapshots. As illustrated in Fig. 11(b), the transmission coefficients of the input metasurface layer were systematically reconfigured across snapshots to generate a series of 2D DFT matrices with orthogonal spatial frequency bins. Fig. 10 compares the spatial frequency spectra obtained from both two-layer and four-layer SIM architectures in dual-target scenarios. The results demonstrate that deeper SIM configurations significantly enhance DFT matrix approximation fidelity, yielding a substantially refined spatial frequency spectrum. Experimental validation confirmed that the SIM, operating at optical computational speeds, achieved an MSE of -40 dB for 2D DOA estimation [31].

Moreover, the architecture of SIM can be scaled to enhance the capability in multi-level diffractive modulation of incident electromagnetic fields [21]. A larger number of meta-atoms per layer translates to an expanded aperture, thereby enabling higher angular resolution in signal detection. Furthermore, increasing the network depth through additional layers allows for the estimation of a substantially higher number of target sources. Unlike conventional angle estimation techniques that impose substantial computational burdens on electronic systems, a SIM performs DOA estimation at the speed of light, making it particularly advantageous for latency-sensitive applications, such as autonomous vehicles and high-speed rail communications. Additionally, when multiple sources are present, the input electromagnetic field comprises a superposition of plane waves arriving from distinct directions. As a result, the DOA estimates are subsequently obtained by identifying the top- K intensity peaks across all detection regions, where K denotes the number of incident signals. Notably, this detection mechanism inherently enables the designed SIM architecture to simultaneously estimate both the angles and the number of target sources [29].

VI. SIM FOR COMPUTING

SIMs have a transformative impact on future computing architectures, opening up new avenues for integrating computing functions into the wireless transmission process. Next, a pair of representative examples are provided for demonstrating its exciting potential way beyond wireless communication and sensing applications.

A. Pattern Generation

Computational imaging is capable of overcoming the limitations of traditional optical imaging techniques [91]. By leveraging a SIM as a front-end, novel imaging capabilities can be achieved by precisely controlling its internal electromagnetic fields and pairing it with appropriate computational algorithms. Building upon this philosophy, Hassan *et al.* [92] established an analytical framework for calculating the received power of signals after passing through a SIM. They further proposed a pair of distinct optimization approaches: a GD method for meta-atoms featuring continuous phase modulation, and a successive refinement technique for those with discrete phase configurations. Their simulation results revealed that a three-layer SIM capable of continuous phase adjustment could concentrate over 90% of radiated power within targeted regions.

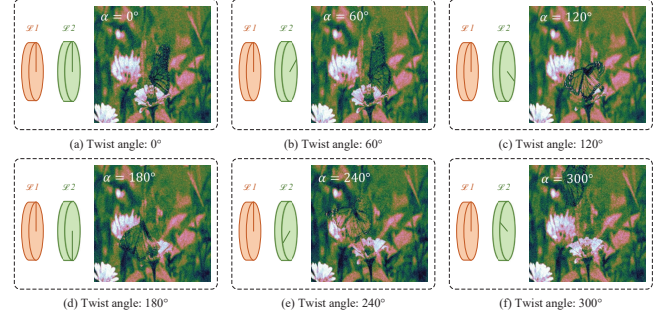


Fig. 12: Holograms generated by a two-layer SIM at six different twist angles.

By contrast, achieving comparable power concentration with binary phase shift meta-atoms necessitated more than five metasurface layers.

To address the substantial challenge of high maintenance costs associated with conventional image storage, Fan *et al.* [93] introduced the concept of metasurface-based disks (meta-disks) that extend the capacity limits of holographic storage by exploiting uncorrelated structural twist angles. This approach enables the storage of large volumes of information through internal structural multiplexing. Utilizing advanced 3D printing technology combined with Pancharatnam-Berry metasurfaces [93], the authors fabricated a twin-layer SIM architecture with an interlayer spacing of $1,000 \mu\text{m}$, where each layer comprises circular disks containing 256 meta-atoms in radius. To demonstrate the SIM's potential for holographic display applications, the temporal information from an original video was encoded into different twist angles between the two meta-disk layers. As illustrated in Fig. 12, high-quality video sequences with a resolution of 200×200 pixels were successfully reconstructed at the designated output plane by sequentially adjusting the metasurface twist angle at intervals of 60° .

This advanced pattern generation technology holds significant promise for next-generation multiple access using holograms and may potentially unlock new possibilities for generative AI applications. Moreover, this method can be utilized to enable semantic information representation, particularly for intricate scene information such as geometric configurations and spatial arrangements, which are difficult to describe accurately using conventional techniques. By using a SIM to directly generate the desired shape and edge at the receiving array, the amount of data traffic could be tremendously reduced [83].

B. Logical Operations

In addition, SIMs offer promising capabilities for implementing logical operations in the spatial domain, which holds substantial potential for future bit-level electromagnetic information processing. A recent experimental demonstration [26] showcased a twin-layer microwave-frequency SIM that successfully realized the three fundamental binary logical operations: AND, OR, and NOT. The architecture employs an input layer comprising a patterned mask with multiple

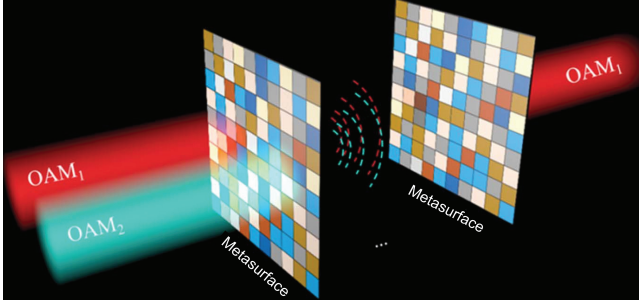


Fig. 13: Schematic of OAM mode logical operation based on SIM .

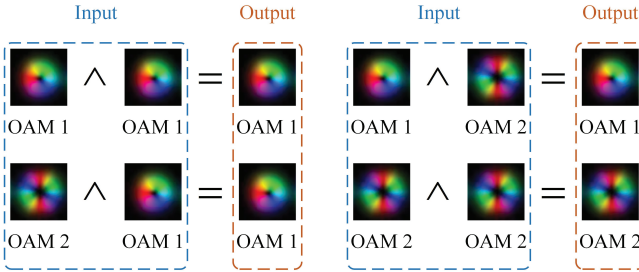


Fig. 14: Illustration of the logic AND gate.

switchable regions, each capable of toggling between high and low transmittance states, where the high transmittance state designates regions activated for logical computation. At the output plane, two distinct regions encode the binary logic states ‘1’ and ‘0’, respectively. Through training the phase modulation of each hidden layer via error backpropagation [26], the SIM achieves precise electromagnetic wave routing to the appropriate output region. Building upon this foundation, Ding *et al.* [94] introduced a novel architecture for optical quantum-domain logical operations leveraging spatial and polarization multiplexing within a SIM framework. In their approach, the pair of quantum states, $|0\rangle$ and $|1\rangle$, are encoded using orthogonal linear polarization states of classical electromagnetic waves. By superimposing these basis states, the optimized SIM successfully executes four fundamental quantum-domain logical operations: the three Pauli gates and the Hadamard gate. Remarkably, the optical quantum operator implemented exhibited exceptional fidelity across all four gates, achieving 99.96% in numerical simulations and 99.88% in experimental validation.

Instead of employing linear momentum states for logic representation that may suffer from ambiguous discrimination boundaries, the authors of [95] introduced an innovative technique of leveraging orbital angular momentum (OAM) modes as logical states. This methodology not only augments the parallel processing capacity attained but also significantly enhances the distinguishability and robustness of logical states, capitalizing on the infinite dimensionality and orthogonality of OAM modes. Through precise manipulation of the phase and amplitude distributions across multiple diffractive layers, the SIM enables independent control of both the modal content and spatial positioning of multiple OAM beams. As illustrated in Fig. 13, two OAM modes incident from distinct

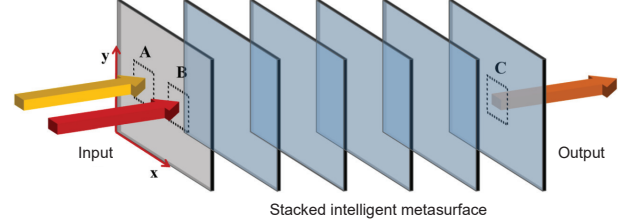


Fig. 15: A schematic of logic gates using polarization DoF based on SIM. Ports A and B on the input layer represent the two inputs, while C represents the output port located at the center of the output layer.

spatial locations serve as input data, and the primary objective of the SIM is to perform independent modulation of these input fields, thus ensuring that the transformations conform to the computational requirements of logical gates. Following wavefront modulation through multiple diffraction screens and subsequent propagation, a vortex beam carrying a single OAM mode emerges at the center of the output plane. Fig. 14 illustrates the OAM-based logic AND gate, where the first and second columns display the intensity distributions of the input beams, with the color gradient from blue to red indicating the OAM mode order. The corresponding outputs are shown in the third column of Fig. 14, which conform to that of the logic AND gate.

In [96], Liu *et al.* developed a SIM architecture that achieves remarkable neuronal density for optical computing, integrating 40,000 neurons within a compact $2\text{ cm} \times 2\text{ cm}$ footprint. To validate this platform, they numerically simulated an optical half-adder employing two metasurface layers and subsequently verified it experimentally in the Terahertz regime. Similarly, the authors of [97] utilized SIM to realize a polarization-encoded logical operation exhibiting high extinction ratios. Their approach harnesses free-space electromagnetic wave propagation and sophisticated engineered interactions with cascaded passive diffractive layers to enable efficient optical computation. As depicted in Fig. 15, they implemented a five-layer architecture capable of executing various logic operations, with constituent pixels featuring dimensions on the order of several hundred nanometers. The binary logical states ‘0’ and ‘1’ are encoded using linearly polarized light beams with electric field orientations along the X and Y directions, respectively, which are injected into the input ports A and B. Upon propagation through the appropriately configured SIM, a linearly polarized beam emerges at output port C, corresponding to the logical states ‘0’ or ‘1’, respectively. By enriching the input encoding patterns and adopting more sophisticated network architectures, SIMs can theoretically realize arbitrary logical functions, presenting promising opportunities for dynamic over-the-air encryption of electromagnetic signals.

VII. FUSION OF COMMUNICATION, SENSING, AND COMPUTING

Emerging application scenarios increasingly necessitate the convergence of communication, sensing, and computing func-

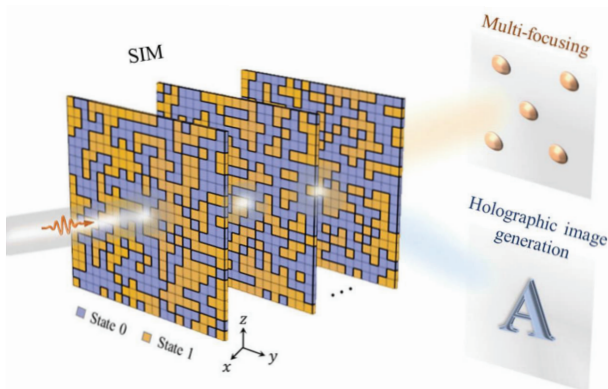


Fig. 16: A schematic showing the dual-functional capability of SIM for achieving multifocusing and holographic imaging.

tionalities within a unified infrastructure. The integration of radar sensing and edge computing capabilities into WiFi and cellular networks, for example, demonstrates considerable potential for efficient radio resource orchestration [21], [28]. This convergence paradigm suggests that a single multifunctional SIM device could simultaneously fulfill these diverse objectives [98]. In this section, we examine existing advances in multiplexing SIM technology to accomplish multiple concurrent tasks.

In [99], Niu *et al.* explored a SIM-enhanced integrated sensing and communication (ISAC) framework, wherein the SIM was configured to produce a tailored beam pattern enabling simultaneous multi-user downlink communication and radar target detection. To achieve this end, the authors formulated an optimization problem aimed at maximizing spectral efficiency subject to directional power constraints, necessitating the joint optimization of the SIM phase shifts and the BS's power allocation. By treating the sensing power constraint as a penalty term within the objective function, they developed and solved the resultant optimization problem using a customized GA algorithm. Following this, Li *et al.* [100] conceived an advanced transmit beamforming technique for SIM-enabled ISAC systems, where they employed a multi-layer beamformer design that maximizes user sum rate, while optimally sculpting the normalized beam pattern for sensing purposes. The resultant non-convex multi-objective optimization problem was addressed through a dual-normalized differential GD algorithm, which leverages gradient differences and dual normalization to strike a flexible trade-off between communication and sensing performance objectives. Furthermore, Jiang *et al.* [101] designed a satellite equipped with SIM to perform dual-function precoding in the wave domain — eliminating the need for conventional digital beamformers — for simultaneously detecting multiple airborne targets, while serving multiple ground-based communication users. A penalty-based GA algorithm was developed for maximizing the communication throughput attained, while maintaining sensing performance.

Recently, Gao *et al.* [29] have demonstrated the significant potential of SIM in RIS-aided mmWave ISAC systems. In contrast to conventional RIS-based communication systems,

where DOA estimation necessitates for the BS to execute a series of computationally intensive operations, including down-conversion, sampling, and digital signal processing, a SIM directly infers angular information from the incident signals and facilitates edge computing. This capability substantially reduces both the power consumption and latency in beam-tracking applications. Specifically, they developed a reflective liquid crystal (LC)-based RIS architecture comprising 20×20 programmable meta-atoms, where each meta-atom achieves 5-bit phase modulation of the incident electromagnetic field through FPGA-controlled supply voltages. By employing a passive SIM to estimate the DOAs of signals originating from both the BS and user, the RIS dynamically optimizes its beamforming configuration to establish a virtual communication link with high-velocity mobile users. Experimental results reveal that the system achieves an average amplitude gain of 17.9 dB at the user's antenna compared to configurations operating without SIM [29].

Moreover, Jia *et al.* [102] explored the potential of using a SIM to support the dual functions of imaging and beam-forming. Specifically, they developed an advanced architecture employing two layers of tunable binary transmissive metasurfaces that are capable of generating complex holographic patterns on a 2D plane. By optimizing the binary phase of each meta-atom to minimize discrepancies between the actual and desired radiation patterns, as illustrated in Fig. 16, this SIM configuration can simultaneously achieve multi-focusing and holographic imaging capabilities, while maintaining a transmission efficiency exceeding 95%.

VIII. KEY TECHNICAL ISSUES RELATED TO SIMS

In this section, we explore the practical challenges of implementing SIMs. Specifically, we cover several key aspects, including channel estimation, antenna selection and user association, inter-layer propagation coefficient calibration, propagation modeling, and EE analysis.

A. Channel Estimation

Accurate channel state information (CSI) is vital for carrying out the desired signal processing function in the wave domain, particularly in dynamic wireless communication systems [21], [103]. Typically, each metasurface layer consists of a large number of meta-atoms, which leads to a situation where the number of RF chains at the BS is much lower than the dimension of channels between the SIM and users. This disparity renders CSI acquisition in SIM-assisted communication systems an under-determined problem. To tackle this issue, Nadeem *et al.* [104] developed a channel estimation technique that collects multiple copies of uplink pilot signals that propagate through the SIM. Orthogonal pilot signals were employed to prevent interference between users. Moreover, they theoretically analyzed the MSE of the channel estimates and applied a GD algorithm to optimize the phase shifts of meta-atoms, aiming for minimizing the MSE. Notably, they also demonstrated that by leveraging the low-rank property of channel correlation matrices [105], the pilot overhead can be significantly reduced.

TABLE VI: A survey of existing channel estimation schemes for SIM-based communication systems.

Reference	Year	Link	Scenario	Estimator	Contributions
Nadeem <i>et al.</i> [104]	2024	UL	MU	MMSE estimator	Leverage GD algorithm to configure the SIM for minimizing MSE
Yao <i>et al.</i> [106]	2024	UL	MU	Subspace-based estimators	Utilize the low-rank characteristics of the channel subspace to improve the estimation performance
Yao <i>et al.</i> [107]	2024	UL	MU	OMP	Utilize the decision mechanism to adaptively determine the sparsity
Ginige <i>et al.</i> [108]	2025	UL	MU	Alternative LS	Use PARAFAC and Tucker methods to represent multidimensional algebraic structures
Lawal <i>et al.</i> [109]	2025	UL	MU	CNN	Learn the internal propagation behavior without explicit physical modeling

Furthermore, Yao *et al.* [106] identified a subspace that spans any spatial correlation matrix when ultra-dense elements are arranged on a metasurface. By relying on realistic partial CSI of the channel statistics, two subspace-based channel estimators were developed for enhancing the estimation accuracy by projecting both conventional least squares (LS) and MMSE estimates into the lower-dimensional subspace they identified. In [107], the same researchers exploited the sparse nature of mmWave channels in the beam domain. They framed the channel estimation problem of SIM-aided mmWave communication systems as a sparse recovery task and applied the popular orthogonal matching pursuit (OMP) algorithm to determine the channel parameters. Additionally, they introduced a soft decision threshold for terminating the OMP iterations when the sparsity is unknown. Recent studies [108] and [109] have also applied alternative LS and convolutional neural networks (CNNs) to address channel estimation challenges in SIM-assisted communication systems. To illustrate, the existing channel estimation techniques conceived for SIM-assisted communication systems are summarized in Table VI.

B. Antenna Selection and User Association

SIM essentially performs specific transformations, as waves propagate through it. For SIM to work effectively, it is crucial to establish bespoke protocols that define the role of each port. The assignment and definition of these ports significantly impact the overall performance. In wireless communication systems, this involves selecting the appropriate antennas and matching them to the right users. To illustrate this concept, let's consider a multiuser transmission scenario, where a SIM is utilized to mitigate interference among multiple users in the wave domain.

- ◊ **Antenna Selection:** As shown in Fig. 17, different antenna selection schemes can influence the capability of SIMs for mitigating inter-user interference. When the antennas are too close to each other, it becomes harder for users to differentiate their individual signals from the superimposed waveforms. Hence, selecting antennas that are spaced far apart enhances the ability to achieve interference-free transmission using the wave-domain beamforming technique.
- ◊ **User Association:** As illustrated in Fig. 18, the choice of the specific user association strategy also affects the performance of wave-domain beamforming. Following the same principle as in classic antenna selection, it is

suggested that neighboring antennas at the BS should transmit signals to two users who are farther apart. This setup allows for achieving effective interference mitigation.

Specifically, when considering a scenario, where a BS with M antennas serves K users, the total number of possible combinations for implementing antenna selection and user association can be expressed as

$$P(M, K) = \frac{M!}{(M - K)!}. \quad (2)$$

Therefore, determining the optimal pairing scheme of antennas to users is an NP-hard problem, necessitating the development of efficient heuristic methods. A similar challenge exists in sensing and computing applications. For instance, in object recognition, the assignment of probes to various image categories can have a significant impact on the classification performance. As such, these assignments must be carefully planned before the practical implementation of SIM.

At the time of writing, research on antenna selection and user association in SIM-aided systems is still in its early stages. In [110], Lin *et al.* investigated the impact of antenna selection on SIM performance in low-Earth orbit (LEO) satellite communications. They developed a user grouping method to manage large numbers of users by dividing them into multiple groups based on channel correlation. Within each group, users are served using spatial division multiple access (SDMA), while different groups are served in separate time slots. To further enhance system performance, the Hungarian algorithm was used at the satellite to optimize antenna selection [110]. In [111], Shi *et al.* examined the AP-UE association in cell-free systems. They employed a greedy algorithm to pair UEs with their nearest APs and then jointly optimized power allocation and wave-based precoding to maximize data rates.

C. Propagation Coefficient Calibration

The deformation of the mechanical support structure during the assembly of the SIM, as well as the bending of the metasurfaces due to their weight, can cause the propagation coefficients $w_{n,\tilde{n}}^l$ between adjacent metasurface layers to deviate from their initial values modelled in (1). This deviation presents challenges during the configuration of the SIM in the training process and may negatively impact its inference performance. Therefore, before implementing the SIM, it is

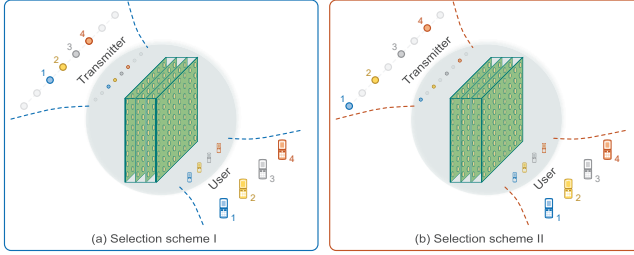


Fig. 17: Illustration of two different antenna selection schemes.

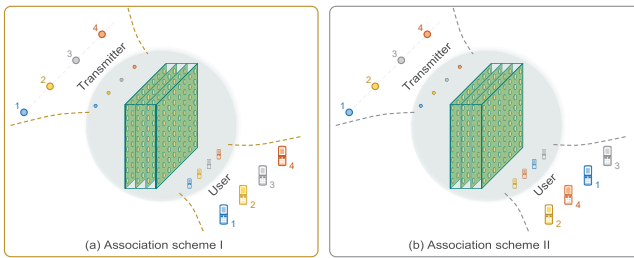


Fig. 18: Illustration of two different user association schemes.

crucial to appropriately calibrate the wave propagation coefficients between adjacent metasurface layers to ensure more reliable training results [14]. In [19], Liu *et al.* utilized 5,000 experimental samples to fine-tune the propagation coefficients by employing the gradient descent method. For each sample, they applied random bias voltages to all the meta-atoms in the SIM and measured the resultant output field patterns using a custom array of 8×8 receiving antennas. After calibrating the propagation coefficients, they found that the measured energy distributions closely matched the simulated ones, demonstrating excellent agreement.

D. Propagation Modeling

Accurate propagation modeling is essential for producing the desired inference results [112]. Given that SIMs rely on the cascaded response of multiple metasurface layers, several recent contributions have been made to characterize the near-field wave propagation within SIMs. In [113], Maryam *et al.* investigated the achievable sum-rate of SIMs in uplink scenarios while accounting for hardware imperfections. The authors formulated a non-convex sum-rate optimization problem and employed genetic algorithms alongside interior point methods to obtain the solution. Evaluating the performance under both Rayleigh fading and 3GPP channel models under constraints on either equal numbers of RF chains or equal physical aperture sizes, they demonstrated that SIMs outperform conventional digital phased arrays, when the number of RF chains is held constant. Building upon this, Nerini *et al.* [114] developed a physically consistent channel model for SIM-aided systems that explicitly incorporates realistic element coupling effects and accounts for metasurfaces having non-diagonal phase shift matrices.

More recently, Abrardo *et al.* [115] proposed a comprehensive optimization framework for heterogeneous SIM architectures that circumvents the restrictive assumptions of

prior approaches. The model they presented is grounded in multi-port network theory for characterizing general electromagnetic collaborative objects (ECOs) and establishes a unified optimization framework. Subsequently, they view SIMs as a specific ECO architecture, providing valuable insights into optimization strategies across various SIM configurations and analyzing the associated computational complexity. The authors further examine the implications of commonly adopted modeling assumptions and introduce a backpropagation-based algorithm for implementing GD optimization in simplified SIM configurations.

E. Energy Efficiency Analysis

Energy loss analysis is critical for validating a SIM's low-power performance in signal processing applications. In [116], Stefan *et al.* investigated the EE performance of SIM-based MIMO broadcast systems. To comprehensively evaluate the potential of a SIM, they examined both dirty paper coding (DPC) and linear precoding schemes, formulating corresponding EE maximization problems for each approach and leveraging the broadcast channel (BC)-multiple-access channel (MAC) duality to derive an equivalent optimization problem. Subsequently, they optimized the users' covariance matrices through successive convex approximation (SCA) based on a tight lower bound of the achievable sum-rate, coupled with Dinkelbach's method. The resultant high-dimensional phase shift optimization problem was solved by using a conventional projected gradient-based approach. In [117], Shi *et al.* examined the integration of SIM into multi-antenna BSs for downlink multi-user communications, presenting a realistic power consumption model for SIM-assisted systems. They employed a quadratic transformation to reformulate the EE maximization problem and proposed an AO-based joint precoding framework. Specifically, an SCA algorithm was adopted for base station precoding design, while wave-based beamforming was tackled using two approaches: a high-performance semidefinite programming (SDP) method and a computationally efficient projected gradient ascent (PGA) algorithm. Notably, their results revealed that although the optimal number of SIM layers differs between EE and spectral efficiency maximization objectives, a configuration of $2 \sim 5$ layers achieves satisfactory performance across both metrics [117].

IX. FUTURE RESEARCH DIRECTIONS

In this section, we identify research opportunities and challenges ahead for further enhancing the inference capabilities and computational power of SIM.

A. Channel Multiplexing

In addition to directly processing the phase and amplitude of input waves, SIMs can tap into all the DoFs exhibited by electromagnetic waves. Various multiplexing schemes, such as polarization, spectrum, and vortex, can be leveraged to expand the number of available channels, as illustrated in Fig. 19.

- ◊ **Polarization:** The subwavelength structures of anisotropic meta-atoms that exhibit polarization-selective

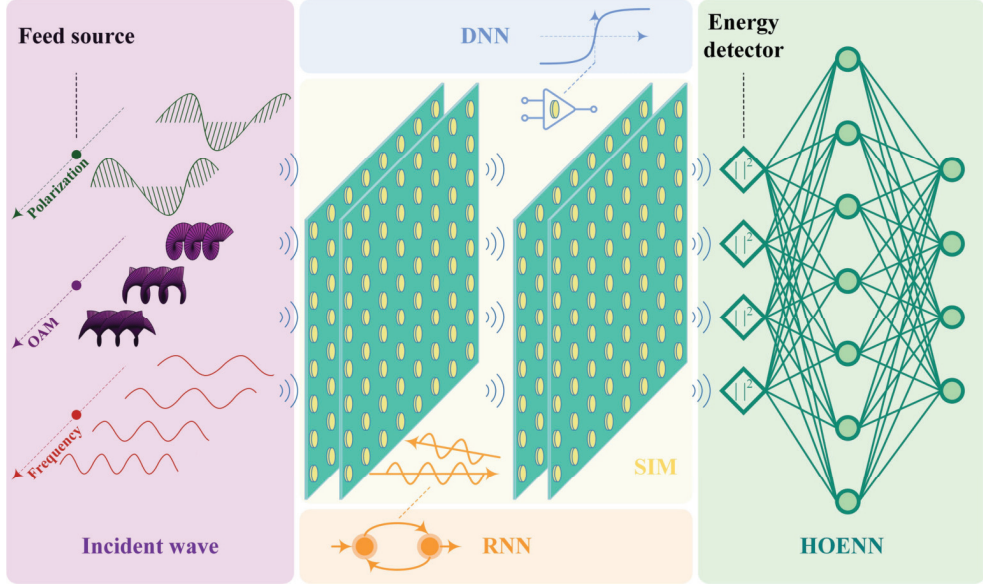


Fig. 19: Schematic of multifunctional SIM, where the number of available channels can be expanded by multiplexing polarization, OAM, and frequencies. In addition, by integrating nonlinear modules, leveraging inter-layer signal reflections, or cascading an electronic network, DNN, RNN, or HOENN can be created to further improve the computing power of SIM.

responses allow for independent, pixel-level control over polarization states [17].

- ◊ **OAM:** Moreover, metasurfaces bestow the unprecedented ability to manipulate structured electromagnetic waves to multiplex information in different OAM channels [15].
- ◊ **Frequency:** Sophisticated meta-atoms also provide unique opportunities for operating across multiple wavelength channels by simultaneously tuning the modulation response and by carefully engineering the native dispersion characteristics of individual meta-atoms on demand [16].

These multiplexing strategies provide distinct advantages in terms of massively increasing the computing scale and degree of parallelism. As a result, a SIM can concurrently perform multiple tasks by processing each channel independently.

B. Structural Parameter Analysis

Similar to an ANN, the representation capability of a SIM is influenced by the number of metasurface layers and the number of meta-atoms per layer. Additionally, the per-layer topology of meta-atoms and inter-layer spacing have an impact on the inference ability of a SIM. Understanding the influence of these hardware parameters is essential for determining the most effective configuration for a practical SIM device.

- ◊ **Number of Layers:** It has been shown that a SIM can approximate any universal linear transformations by performing cascaded complex-valued matrix operations with arbitrarily small error [15]. The dimensionality of the space for linear transformations that can be processed by a SIM is linearly proportional to the number of metasurface layers. In general, deep architectures comprising a larger number of metasurface layers are capable of extracting better features compared to shallow ones. However, they also suffer from increased material absorption

and surface back reflections, which drastically degrade the power efficiency. Therefore, the fundamental tradeoff between inference accuracy and power efficiency makes the use of a massive number of cascaded metasurface layers challenging.

- ◊ **Number of Meta-atoms:** Employing more meta-atoms within each layer can improve the performance of a SIM. However, the law of diminishing returns holds, as the meta-atoms located far from the paraxial region have a negligible impact on the desired input-output transformations.
- ◊ **Per-layer Topology:** Periodic metasurface designs may result in redundant propagation paths within a SIM. Hence, altering the topology of subwavelength meta-atoms can introduce additional flexibility to tune the transfer function of a SIM. Designing sophisticated meta-atom patterns and sparse interconnections could enhance the performance for a given number of meta-atoms or achieve desired functionalities with a more efficient SIM architecture [118].
- ◊ **Inter-layer Spacing:** The connectivity within a SIM can also be controlled by adjusting the distance between metasurface layers using micro-electromechanical systems. Alternatively, the effective path length between metasurface layers can be tailored by tuning the refractive index of phase-changing materials without changing the physical distances.

In a nutshell, designing an effective SIM requires carefully balancing these fundamental tradeoffs, which remains an open challenge.

C. Neural Network Architecture

The concept of neural networks has been utilized for explaining the operating principles of SIMs. However, a SIM

does not inherently include any non-linearity, except for the receiving detector. This limitation may degrade the ability of SIM to extract complex features and handle challenging tasks. As illustrated in Fig. 19, three potential directions can be explored for further enhancing the inference capabilities of SIM:

- ◊ **DNN:** Developing materials and meta-atom designs that exhibit nonlinear responses would be critical for creating authentic DNNs. The inference accuracy of SIMs could benefit from directly integrating a nonlinear module into the meta-atoms. For instance, by altering the voltages applied to the varactor, a programmable activation function can be obtained by detecting the input intensity and by feeding back the threshold to an amplifier in each meta-atom [118]. However, this demands appropriate modeling of the electromagnetic responses and a scalable as well as power-efficient design.
- ◊ **HOENN:** The cascade of a SIM (optical network) and a shallow electronic ANN could create a hybrid optical-electronic neural network (HOENN) having improved performance [16]. A SIM can convert phase-encoded information into intensity patterns, and then energy-efficient energy detectors can act as activation functions for enhancing the inference capability of HOENNs.
- ◊ **RNN:** Existing SIM designs typically use anti-reflective coatings to suppress back-and-forth reflection losses within the SIM [17]. However, taking advantage of these inter-layer reflections could enable the design of recurrent neural networks (RNNs), significantly improving the inference capability of SIMs. Characterizing the coupling between densely packed metasurface layers is quite challenging, as it depends on the configuration of other metasurface layers.

X. CONCLUSIONS

SIM technology holds the promise of supporting analog electromagnetic signal processing at the speed of light. In this overview, we have discussed recent advances in SIM research and development. Beginning with the fundamental principles behind SIM, we have reviewed the substantial progress made in fabricating SIMs for various inference tasks across communication, sensing, and computing applications. We have also unveiled a wealth of new opportunities that could further enhance the computing capability of SIMs and have identified key challenges that still have to be addressed. In summary, SIM has the potential to revolutionize interdisciplinary research at the intersection of electromagnetism, AI, and metamaterials science. Taking advantage of the complementary nature of these emerging technologies may significantly advance all these fields.

REFERENCES

- [1] Y. LeCun, Y. Bengio, and G. Hinton, “Deep learning,” *Nature*, vol. 521, no. 7553, pp. 436–444, May 2015.
- [2] C. Szegedy, V. Vanhoucke, S. Ioffe, J. Shlens, and Z. Wojna, “Rethinking the inception architecture for computer vision,” in *Proc. IEEE Conf. Computer Vision, Pattern Recognition (CVPR)*, 2016, pp. 2818–2826.
- [3] G. Hinton, L. Deng, D. Yu, G. E. Dahl, A.-r. Mohamed, N. Jaitly, A. Senior, V. Vanhoucke, P. Nguyen, T. N. Sainath, and B. Kingsbury, “Deep neural networks for acoustic modeling in speech recognition: The shared views of four research groups,” *IEEE Signal Process. Mag.*, vol. 29, no. 6, pp. 82–97, Nov. 2012.
- [4] D. W. Otter, J. R. Medina, and J. K. Kalita, “A survey of the usages of deep learning for natural language processing,” *IEEE Trans. Neural Netw. Learning Systems*, vol. 32, no. 2, pp. 604–624, Feb. 2021.
- [5] V. Sze, Y.-H. Chen, T.-J. Yang, and J. S. Emer, “Efficient processing of deep neural networks: A tutorial and survey,” *Proc. IEEE*, vol. 105, no. 12, pp. 2295–2329, Dec. 2017.
- [6] A. Silva, F. Monticone, G. Castaldi, V. Galdi, A. Alù, and N. Engheta, “Performing mathematical operations with metamaterials,” *Science*, vol. 343, no. 6167, pp. 160–163, Jan. 2014.
- [7] D. C. Tzorouinis, B. Edwards, and N. Engheta, “Programmable wave-based analog computing machine: a metasurface that designs metasurfaces,” *Nature Commun.*, vol. 16, no. 1, p. 908, Jan. 2025.
- [8] T. J. Cui, M. Q. Qi, X. Wan, J. Zhao, and Q. Cheng, “Coding metamaterials, digital metamaterials and programmable metamaterials,” *Light: Science & Applications*, vol. 3, no. 10, pp. e218–e218, Oct. 2014.
- [9] Q. Cheng, L. Zhang, J. Y. Dai, W. Tang, J. C. Ke, S. Liu, J. C. Liang, S. Jin, and T. J. Cui, “Reconfigurable intelligent surfaces: Simplified-architecture transmitters—from theory to implementations,” *Proc. IEEE*, vol. 110, no. 9, pp. 1266–1289, Sep. 2022.
- [10] J. An, C. Yuen, M. D. Renzo, M. Debbah, H. V. Poor, and L. Hanzo, “Flexible intelligent metasurfaces for downlink multiuser MISO communications,” *IEEE Trans. Wireless Commun.*, vol. 24, no. 4, pp. 2940–2955, Apr. 2025.
- [11] M. Di Renzo, F. H. Danufane, and S. Tretyakov, “Communication models for reconfigurable intelligent surfaces: From surface electromagnetics to wireless networks optimization,” *Proc. IEEE*, vol. 110, no. 9, pp. 1164–1209, Sep. 2022.
- [12] M. Di Renzo, A. Zappone, M. Debbah, M.-S. Alouini, C. Yuen, J. de Rosny, and S. Tretyakov, “Smart radio environments empowered by reconfigurable intelligent surfaces: How it works, state of research, and the road ahead,” *IEEE J. Sel. Areas Commun.*, vol. 38, no. 11, pp. 2450–2525, Nov. 2020.
- [13] G. C. Alexandropoulos, K. Stylianopoulos, C. Huang, C. Yuen, M. Benis, and M. Debbah, “Pervasive machine learning for smart radio environments enabled by reconfigurable intelligent surfaces,” *Proc. IEEE*, vol. 110, no. 9, pp. 1494–1525, Sep. 2022.
- [14] J. An, M. Debbah, T. J. Cui, Z. N. Chen, and C. Yuen, “Emerging technologies in intelligent metasurfaces: Shaping the future of wireless communications,” pp. 1–16, 2025, Early Access.
- [15] X. Lin, Y. Rivenson, N. T. Yardimci, M. Veli, Y. Luo, M. Jarrahi, and A. Ozcan, “All-optical machine learning using diffractive deep neural networks,” *Science*, vol. 361, no. 6406, pp. 1004–1008, Jul. 2018.
- [16] J. Li, D. Mengu, N. T. Yardimci, Y. Luo, X. Li, M. Veli, Y. Rivenson, M. Jarrahi, and A. Ozcan, “Spectrally encoded single-pixel machine vision using diffractive networks,” *Science Advances*, vol. 7, no. 13, p. eabd7690, Mar. 2021.
- [17] X. Luo, Y. Hu, X. Ou, X. Li, J. Lai, N. Liu, X. Cheng, A. Pan, and H. Duan, “Metasurface-enabled on-chip multiplexed diffractive neural networks in the visible,” *Light: Science & Applications*, vol. 11, no. 1, p. 158, May 2022.
- [18] H. Chen, S. Lou, Q. Wang, P. Huang, H. Duan, and Y. Hu, “Diffractive deep neural networks: Theories, optimization, and applications,” *Applied Physics Reviews*, vol. 11, no. 2, Jun. 2024.
- [19] C. Liu, Q. Ma, Z. J. Luo, Q. R. Hong, Q. Xiao, H. C. Zhang, L. Miao, W. M. Yu, Q. Cheng, L. Li *et al.*, “A programmable diffractive deep neural network based on a digital-coding metasurface array,” *Nature Electronics*, vol. 5, no. 2, pp. 113–122, Feb. 2022.
- [20] J. An, C. Xu, D. W. K. Ng, G. C. Alexandropoulos, C. Huang, C. Yuen, and L. Hanzo, “Stacked intelligent metasurfaces for efficient holographic MIMO communications in 6G,” *IEEE J. Sel. Areas Commun.*, vol. 41, no. 8, pp. 2380–2396, Aug. 2023.
- [21] J. An, C. Yuen, C. Xu, H. Li, D. W. K. Ng, M. Di Renzo, M. Debbah, and L. Hanzo, “Stacked intelligent metasurface-aided MIMO transceiver design,” *IEEE Wireless Commun.*, vol. 31, no. 4, pp. 123–131, Aug. 2024.
- [22] H. Liu, J. An, X. Jia, L. Gan, G. K. Karagiannidis, B. Clerckx, M. Benis, M. Debbah, and T. J. Cui, “Stacked intelligent metasurfaces for wireless communications: Applications and challenges,” *IEEE Wireless Commun.*, vol. 32, no. 4, pp. 46–53, Aug. 2025.
- [23] M. Born and E. Wolf, *Principles of optics: electromagnetic theory of propagation, interference and diffraction of light*. Elsevier, 2013.

- [24] S. Mehrabkhani and T. Schneider, "Is the rayleigh-sommerfeld diffraction always an exact reference for high speed diffraction algorithms?" *Optics Express*, vol. 25, no. 24, pp. 30 229–30 240, Nov. 2017.
- [25] M. Di Renzo, "State of the art on stacked intelligent metasurfaces communication, sensing and computing in the wave domain," in *2025 19th European Conf. Antennas, Propag. (EuCAP)*, 2025, pp. 1–3.
- [26] C. Qian, X. Lin, X. Lin, J. Xu, Y. Sun, E. Li, B. Zhang, and H. Chen, "Performing optical logic operations by a diffractive neural network," *Light: Science & Applications*, vol. 9, no. 1, p. 59, Apr. 2020.
- [27] Z. Gu, Q. Ma, X. Gao, J. W. You, and T. J. Cui, "Classification of metal handwritten digits based on microwave diffractive deep neural network," *Advanced Optical Materials*, vol. 12, no. 7, p. 2301938, Oct. 2024.
- [28] Z. Wang, H. Liu, J. Zhang, R. Xiong, K. Wan, X. Qian, M. Di Renzo, and R. C. Qiu, "Multi-user ISAC through stacked intelligent metasurfaces: New algorithms and experiments," *Proc. IEEE Global Commun. Conf. (GLOBECOM)*, pp. 4442–4447, 2024.
- [29] S. Gao, H. Chen, Y. Wang, Z. Duan, H. Zhang, Z. Sun, Y. Shen, and X. Lin, "Super-resolution diffractive neural network for all-optical direction of arrival estimation beyond diffraction limits," *Light: Science & Applications*, vol. 13, no. 1, p. 161, Jul. 2024.
- [30] Z. Guo, Z. Tan, X. Zang, T. Zhang, G. Wang, H. Li, Y. Wang, Y. Zhu, F. Ding, and S. Zhuang, "Polarization-selective unidirectional and bidirectional diffractive neural networks for information security and sharing," *Nature Commun.*, vol. 16, no. 1, p. 4492, May 2025.
- [31] J. An, C. Yuen, Y. L. Guan, M. D. Renzo, M. Debbah, H. V. Poor, and L. Hanzo, "Two-dimensional direction-of-arrival estimation using stacked intelligent metasurfaces," *IEEE J. Sel. Areas Commun.*, vol. 42, no. 10, pp. 2786–2802, Oct. 2024.
- [32] T. Zhou, L. Fang, T. Yan, J. Wu, Y. Li, J. Fan, H. Wu, X. Lin, and Q. Dai, "In situ optical backpropagation training of diffractive optical neural networks," *Photonics Research*, vol. 8, no. 6, pp. 940–953, 2020.
- [33] Z. Zheng, Z. Duan, H. Chen, R. Yang, S. Gao, H. Zhang, H. Xiong, and X. Lin, "Dual adaptive training of photonic neural networks," *Nature Machine Intelligence*, vol. 5, no. 10, pp. 1119–1129, Sep. 2023.
- [34] A. Momeni, B. Rahmani, B. Scellier, L. G. Wright, P. L. McMahon, C. C. Wanjura, Y. Li, A. Skalli, N. G. Berloff, T. Onodera *et al.*, "Training of physical neural networks," *Nature*, vol. 645, no. 8079, pp. 53–61, Sep. 2025.
- [35] D. Tse and P. Viswanath, *Fundamentals of wireless communication*. Cambridge university press, 2005.
- [36] J. An, M. Di Renzo, M. Debbah, and C. Yuen, "Stacked intelligent metasurfaces for multiuser beamforming in the wave domain," in *Proc. IEEE Int. Conf. Commun. (ICC)*, 2023, pp. 2834–2839.
- [37] J. An, M. Di Renzo, M. Debbah, H. Vincent Poor, and C. Yuen, "Stacked intelligent metasurfaces for multiuser downlink beamforming in the wave domain," *IEEE Trans. Wireless Commun.*, vol. 24, no. 7, pp. 5525–5538, Jul. 2025.
- [38] A. Goldsmith, S. Jafar, N. Jindal, and S. Vishwanath, "Capacity limits of MIMO channels," *IEEE J. Sel. Areas Commun.*, vol. 21, no. 5, pp. 684–702, Jun. 2003.
- [39] Q. Spencer, A. Swindlehurst, and M. Haardt, "Zero-forcing methods for downlink spatial multiplexing in multiuser MIMO channels," *IEEE Trans. Signal Process.*, vol. 52, no. 2, pp. 461–471, Feb. 2004.
- [40] H. Q. Ngo, A. Ashikhmin, H. Yang, E. G. Larsson, and T. L. Marzetta, "Cell-free massive MIMO versus small cells," *IEEE Trans. Wireless Commun.*, vol. 16, no. 3, pp. 1834–1850, Mar. 2017.
- [41] E. Shi, J. Zhang, Y. Zhu, J. An, C. Yuen, and B. Ai, "Uplink performance of stacked intelligent metasurface-enhanced cell-free massive MIMO systems," *IEEE Trans. Wireless Commun.*, vol. 24, no. 5, pp. 3731–3746, 2025, Early Access.
- [42] H. Boleskei, D. Gesbert, and A. Paulraj, "On the capacity of OFDM-based spatial multiplexing systems," *IEEE Trans. Commun.*, vol. 50, no. 2, pp. 225–234, Feb. 2002.
- [43] Z. Li, J. An, and C. Yuen, "Stacked intelligent metasurfaces-enhanced MIMO OFDM wideband communication systems," *IEEE Trans. Wireless Commun.*, pp. 1–16, 2025, Early Access.
- [44] E. E. Bahingayi, N. Stefan Perović, and L.-N. Tran, "Scaling achievable rates in SIM-aided MIMO systems with metasurface layers: A hybrid optimization framework," pp. 2773–2777, Sep. 2025.
- [45] A. Papazafeiropoulos, J. An, P. Kourtessis, T. Ratnarajah, and S. Chatzinotas, "Achievable rate optimization for stacked intelligent metasurface-assisted holographic MIMO communications," *IEEE Trans. Wireless Commun.*, vol. 23, no. 10, pp. 13 173–13 186, Oct. 2024.
- [46] N. Stefan Perović and L.-N. Tran, "Mutual information optimization for SIM-based holographic MIMO systems," *IEEE Commun. Lett.*, vol. 28, no. 11, pp. 2583–2587, 2024.
- [47] H. Liu, J. An, G. C. Alexandropoulos, D. W. K. Ng, C. Yuen, and L. Gan, "Multi-user MISO with stacked intelligent metasurfaces: A DRL-based sum-rate optimization approach," *IEEE Trans. Cog. Commun. Netw.*, pp. 1–16, 2025, Early Access.
- [48] X. Yang, J. Zhang, E. Shi, Z. Liu, J. Liu, K. Zheng, and B. Ai, "Joint SIM configuration and power allocation for stacked intelligent metasurface-assisted MU-MISO systems with TD3," in *Proc. IEEE Global Commun. Conf. (GLOBECOM)*, 2024, pp. 3255–3260.
- [49] A. Papazafeiropoulos, P. Kourtessis, S. Chatzinotas, D. I. Kaklamani, and I. S. Venieris, "Achievable rate optimization for large stacked intelligent metasurfaces based on statistical CSI," *IEEE Wireless Commun. Lett.*, vol. 13, no. 9, pp. 2337–2341, Sep. 2024.
- [50] D. Darsena, F. Verde, I. Judice, and V. Galdi, "Design of stacked intelligent metasurfaces with reconfigurable amplitude and phase for multiuser downlink beamforming," *IEEE Open J. Commun. Society*, vol. 6, no. 1, pp. 531–550, Jan. 2025.
- [51] A. Mohammadzadeh, H. Zarini, M. R. Mili, M. J. Siavoshani, A. Movaghfar, J. An, and N. Al-Dhahir, "Meta reinforcement learning empowered orchestration of SIM and RIS for downlink multiuser communications," *arXiv preprint*, 2024.
- [52] H. Zarini, J. An, M. Sookhak, and E. Basar, "Interplay of STAR-RIS and SIM: Joint computing and communication for full-space coverage," *arXiv preprint*, 2024.
- [53] J. Fang, C. Zhang, J. An, H. Yu, Q. Wu, M. Debbah, and C. Yuen, "Stacked intelligent metasurface assisted multiuser communications: From a rate fairness perspective," *IEEE Trans. Commun.*, pp. 1–16, 2025, Early Access.
- [54] H. Zarini, S. M. Kazemi, J. An, A. Movaghfar, S. Hessabi, and M. Sookhak, "QoE-driven resource allocation for stacked intelligent metasurface systems," *arXiv*, 2024.
- [55] ———, "On the application of active RIS to stacked intelligent metasurface systems," *arXiv*, 2024.
- [56] A. Papazafeiropoulos, P. Kourtessis, S. Chatzinotas, D. I. Kaklamani, and I. S. Venieris, "Performance of double-stacked intelligent metasurface-assisted multiuser massive MIMO communications in the wave domain," *IEEE Trans. Wireless Commun.*, vol. 24, no. 5, pp. 4205–4218, May 2025.
- [57] H. Zarini, S. M. Kazemi, J. An, M. Sookhak, and J. Choi, "On the orchestration of SIM and UAV," in *Proc. IEEE Int. Conf. Commun. (ICC)*, 2025, pp. 2913–2918.
- [58] K. Xiong, Z. Chen, J. Xie, Y. Qin, S. Leng, and C. Yuen, "Digital twin-based SIM communication and flight control for advanced air mobility," *IEEE Trans. Netw. Science Engineer.*, vol. 13, no. 1, pp. 728–744, Jan. 2026.
- [59] H. Niu, X. Lei, J. An, L. Zhang, and C. Yuen, "On the efficient design of stacked intelligent metasurfaces for secure SISO transmission," *IEEE Trans. Inf. Forensics Security*, vol. 20, pp. 60–70, Nov. 2025.
- [60] E. E. Bahingayi, S. Lin, M. Uysal, M. Di Renzo, and L.-N. Tran, "A refined alternating optimization for sum rate maximization in SIM-aided multiuser MISO systems," *IEEE Wireless Commun. Lett.*, vol. 15, no. 1, pp. 1250–1254, Dec. 2026.
- [61] J. An, C. Yuen, L. Dai, M. Di Renzo, M. Debbah, and L. Hanzo, "Near-field communications: Research advances, potential, and challenges," *IEEE Wireless Commun.*, vol. 31, no. 3, pp. 100–107, Jun. 2024.
- [62] Q. Li, M. El-Hajjar, C. Xu, J. An, C. Yuen, and L. Hanzo, "Stacked intelligent metasurface-based transceiver design for near-field wideband systems," *IEEE Trans. Commun.*, vol. 73, no. 9, pp. 8125–8139, Sep. 2025.
- [63] X. Jia, J. An, H. Liu, L. Gan, M. Di Renzo, M. Debbah, and C. Yuen, "Stacked intelligent metasurface enabled near-field multiuser beamfocusing in the wave domain," in *Proc. IEEE 99th Veh. Technol. Conf. (VTC2024-Spring)*, 2024, pp. 1–5.
- [64] A. Papazafeiropoulos, P. Kourtessis, S. Chatzinotas, D. I. Kaklamani, and I. S. Venieris, "Near-field beamforming for stacked intelligent metasurfaces-assisted MIMO networks," *IEEE Wireless Commun. Lett.*, vol. 13, no. 11, pp. 3035–3039, Nov. 2024.
- [65] S. Park, A. Alkhateeb, and R. W. Heath, "Dynamic subarrays for hybrid precoding in wideband mmwave MIMO systems," *IEEE Trans. Wireless Commun.*, vol. 16, no. 5, pp. 2907–2920, May 2017.
- [66] A. Ming, J. An, L. Gan, A. Nallanathan, and N. Al-Dhahir, "Flexible intelligent metasurface for mitigating beam squint in wideband communications," *IEEE Trans. Veh. Technol.*, pp. 1–6, 2025, Early Access.

- [67] Z. Li, J. An, and C. Yuen, "Stacked intelligent metasurface-enhanced wideband multiuser MIMO OFDM-IM communications," *arXiv preprint arXiv:2509.22327*, 2025.
- [68] E. Shi, J. Zhang, H. Du, B. Ai, C. Yuen, D. Niyato, K. B. Letaief, and X. Shen, "RIS-aided cell-free massive MIMO systems for 6G: Fundamentals, system design, and applications," *Proc. IEEE*, vol. 112, no. 4, pp. 331–364, Sep. 2024.
- [69] Y. Hu, J. Zhang, E. Shi, Y. Lu, J. An, C. Yuen, and B. Ai, "Joint beamforming and power allocation design for stacked intelligent metasurfaces-aided cell-free massive MIMO systems," *IEEE Trans. Veh. Technol.*, vol. 74, no. 3, pp. 5235–5240, Mar. 2025.
- [70] E. Shi, J. Zhang, Y. Zhu, Z. Liu, J. An, C. Yuen, and B. Ai, "Uplink performance and beamforming design of sim-enhanced cell-free massive MIMO systems," in *Proc. IEEE VTS Asia Pacific Wireless Commun. Symposium (APWCS)*, 2024, pp. 01–05.
- [71] Q. Li, M. El-Hajjar, C. Xu, J. An, C. Yuen, and L. Hanzo, "Stacked intelligent metasurfaces for holographic MIMO-aided cell-free networks," *IEEE Trans. Commun.*, vol. 72, no. 11, pp. 7139–7151, Nov. 2024.
- [72] E. Park, S.-H. Park, O. Simeone, M. D. Renzo, and S. Shamai, "SIM-enabled hybrid digital-wave beamforming for fronthaul-constrained cell-free massive MIMO systems," *IEEE Trans. Wireless Commun.*, pp. 1–16, 2025, Early Access.
- [73] H. Liu, J. An, D. W. K. Ng, G. C. Alexandropoulos, and L. Gan, "DRL-based orchestration of multi-user MISO systems with stacked intelligent metasurfaces," in *Proc. IEEE Int. Conf. Commun. (ICC)*, 2024, pp. 4991–4996.
- [74] L.-H. Hoang, M.-H. Pham, Q.-T. Luu, and V.-D. Nguyen, "Secure multiuser communications with stacked intelligent metasurfaces using quantum reinforcement learning," in *Proc. Int. Conf. Advanced Technol. Commun. (ATC)*, 2025, pp. 1–6.
- [75] X. Yang, J. Zhang, E. Shi, C. Yuen, and B. Ai, "Low-complexity phase shift and power optimization for stacked intelligent metasurface communications with meta-learning," *IEEE Trans. Veh. Technol.*, pp. 1–6, 2025, Early Access.
- [76] C. Liu, K. Qiao, R. Jiang, and W. Yuan, "Sum rate maximization for reconfigurable intelligent surface-aided SIM-RSMA system," *IEEE Commun. Lett.*, pp. 1–5, 2025, Early Access.
- [77] Y. Sun, K. An, M. Yu, Y. Hu, Y. Zhu, Z. Lin, M. Xiao, N. Al-Dhahir, D. Niyato, and J. Wang, "Dual-polarized stacked metasurface transceiver design with rate splitting for next-generation wireless networks," *IEEE J. Sel. Areas Commun.*, vol. 43, no. 3, pp. 811–833, Mar. 2025.
- [78] H. Niu, J. An, L. Zhang, X. Lei, and C. Yuen, "Enhancing physical layer security for siso systems using stacked intelligent metasurfaces," in *Proc. IEEE VTS Asia Pacific Wireless Commun. Symposium (APWCS)*, 2024, pp. 1–5.
- [79] K. Yu, J. Xie, Q. Cui, X. Lv, B. Chen, P. Wang, Y. Wang, and X. Tao, "Energy efficient design for SIM-NOMA enabled satellite beam-hopping system," *IEEE Trans. Aerospace Electro. Systems*, pp. 1–10, 2025, Early Access.
- [80] M. Amiri, S. Javadi, H. Zarini, M. R. Mili, J. An, M. Sookhak, and I. Krikidis, "Stacked intelligent metasurface for simultaneous wireless information and power transfer," in *Proc. IEEE Int. Conf. Commun. (ICC)*, 2025, pp. 4583–4588.
- [81] G. Huang, J. An, Z. Yang, L. Gan, M. Bennis, and M. Debbah, "Stacked intelligent metasurfaces for task-oriented semantic communications," *IEEE Wireless Commun. Lett.*, vol. 14, no. 2, pp. 310–314, Feb. 2025.
- [82] H. Liu, J. An, Q. Ma, L. Gan, M. Bennis, M. Debbah, and T. J. Cui, "A novel hybrid optical-electronic neural network approach to task-oriented semantic communications," in *Proc. IEEE Int. Conf. Commun. (ICC)*, 2025, pp. 2418–2423.
- [83] G. Huang, J. An, L. Gan, D. Niyato, M. Debbah, and T. Jun Cui, "Stacked intelligent metasurfaces for multi-modal semantic communications," *IEEE Wireless Commun. Lett.*, vol. 14, no. 9, pp. 2828–2832, Sep. 2025.
- [84] M. Hua, C. Bian, H. Wu, and D. Gunduz, "Implementing neural networks over-the-air via reconfigurable intelligent surfaces," *arXiv preprint arXiv:2508.01840*, 2025.
- [85] M. Huang, R. Li, Y. Zou, B. Zheng, C. Qian, H. Jin, and H. Chen, "A comprehensive review of metasurface-assisted direction-of-arrival estimation," *Nanophotonics*, vol. 13, no. 24, pp. 4381–4396, Oct. 2024.
- [86] S. Lin, J. An, L. Gan, and M. Debbah, "UAV-mounted SIM: A hybrid optical-electronic neural network for DoA estimation," in *Proc. IEEE Int. Conf. Acoustics, Speech, Signal Process. (ICASSP)*, 2025, Early Access, pp. 1–5.
- [87] H. V. Poor, *An introduction to signal detection and estimation*. Springer Science & Business Media, 2013.
- [88] M. Huang, B. Zheng, R. Li, X. Li, Y. Zou, T. Cai, and H. Chen, "Diffraction neural network for multi-source information of arrival sensing," *Laser & Photonics Reviews*, vol. 17, no. 10, p. 2300202, 2023.
- [89] J. An, C. Yuen, Y. L. Guan, M. Di Renzo, M. Debbah, H. V. Poor, and L. Hanzo, "Stacked intelligent metasurface performs a 2D DFT in the wave domain for DOA estimation," in *ICC 2024 - IEEE Int. Conf. Commun.*, 2024, pp. 3445–3451.
- [90] A. Javed, N. U. Hassan, M. D. Renzo, and C. Yuen, "SIM-IPS: Stacked intelligent metasurface-based indoor positioning system," *IEEE Open J. Commun. Society*, vol. 6, no. 1, pp. 3528–3542, Apr. 2025.
- [91] J. N. Mait, G. W. Euliss, and R. A. Athale, "Computational imaging," *Advances in Optics and Photonics*, vol. 10, no. 2, pp. 409–483, May 2018.
- [92] N. U. Hassan, J. An, M. Di Renzo, M. Debbah, and C. Yuen, "Efficient beamforming and radiation pattern control using stacked intelligent metasurfaces," *IEEE Open J. Commun. Society*, vol. 5, pp. 599–611, Jan. 2024.
- [93] Z. Fan, C. Qian, Y. Jia, Y. Feng, H. Qian, E.-P. Li, R. Fleury, and H. Chen, "Holographic multiplexing metasurface with twisted diffractive neural network," *Nature Commun.*, vol. 15, no. 1, p. 9416, Oct. 2024.
- [94] X. Ding, Z. Zhao, P. Xie, D. Cai, F. Meng, C. Wang, Q. Wu, J. Liu, S. N. Burokur, and G. Hu, "Metasurface-based optical logic operators driven by diffractive neural networks," *Advanced Materials*, vol. 36, no. 9, p. 2308993, Nov. 2024.
- [95] P. Wang, W. Xiong, Z. Huang, Y. He, Z. Xie, J. Liu, H. Ye, Y. Li, D. Fan, and S. Chen, "Orbital angular momentum mode logical operation using optical diffractive neural network," *Photonics Research*, vol. 9, no. 10, pp. 2116–2124, Oct. 2021.
- [96] Y. Liu, W. Chen, X. Wang, and Y. Zhang, "All dielectric metasurface based diffractive neural networks for 1-bit adder," *Nanophotonics*, vol. 13, no. 8, pp. 1449–1458, Jan. 2024.
- [97] X. Lin, K. Zhang, K. Liao, H. Huang, Y. Fu, X. Zhang, S. Feng, and X. Hu, "Polarization-based all-optical logic gates using diffractive neural networks," *Journal of Optics*, vol. 26, no. 3, p. 035701, Feb. 2024.
- [98] A. Fadakar and A. F. Molisch, "Stacked intelligent metasurfaces for multicarrier cognitive radio ISAC," *arXiv preprint arXiv:2511.13933*, 2025.
- [99] H. Niu, J. An, A. Papazafeiropoulos, L. Gan, S. Chatzinotas, and M. Debbah, "Stacked intelligent metasurfaces for integrated sensing and communications," *IEEE Wireless Commun. Lett.*, vol. 13, no. 10, pp. 2807–2811, Oct. 2024.
- [100] S. Li, F. Zhang, T. Mao, R. Na, Z. Wang, and G. K. Karagiannidis, "Transmit beamforming design for ISAC with stacked intelligent metasurfaces," *IEEE Trans. Veh. Technol.*, vol. 74, no. 4, pp. 6767–6772, Apr. 2025.
- [101] C. Jiang, H. Yuan, C. Zhang, J. An, C. Huang, and C. Yuen, "Stacked intelligent metasurface-enabled satellite integrated sensing and communications systems," *IEEE Wireless Commun. Lett.*, pp. 1–5, 2025, Early Access.
- [102] Y. Jia, H. Lu, Z. Fan, B. Wu, F. Qu, M.-J. Zhao, C. Qian, and H. Chen, "High-efficiency transmissive tunable metasurfaces for binary cascaded diffractive layers," *IEEE Trans. Antennas Propag.*, vol. 72, no. 5, pp. 4532–4540, May 2024.
- [103] X. Dong, C. Chen, G. Yu, L. Zhou, C. Yuan, and J. Zhang, "Deep learning-based channel estimation for stacked intelligent metasurface-enhanced multi-user communications," *IEEE Trans. Veh. Technol.*, pp. 1–6, 2026, Early Access.
- [104] Q.-U.-A. Nadeem, J. An, and A. Chaaban, "Hybrid digital-wave domain channel estimator for stacked intelligent metasurface enabled multi-user MISO systems," in *2024 IEEE Wireless Commun. Netw. Conf. (WCNC)*, 2024, pp. 1–6.
- [105] J. An, C. Yuen, C. Huang, M. Debbah, H. Vincent Poor, and L. Hanzo, "A tutorial on holographic MIMO communications—Part I: Channel modeling and channel estimation," *IEEE Commun. Lett.*, vol. 27, no. 7, pp. 1664–1668, Jul. 2023.
- [106] X. Yao, J. An, L. Gan, M. Di Renzo, and C. Yuen, "Channel estimation for stacked intelligent metasurface-assisted wireless networks," *IEEE Wireless Commun. Lett.*, vol. 13, no. 5, pp. 1349–1353, May 2024.
- [107] X. Yao, J. An, G. Huang, H. Liu, L. Gan, and C. Yuen, "Sparse channel estimation for stacked intelligent metasurface-assisted mmwave communications," in *Proc. IEEE VTS Asia Pacific Wireless Commun. Symposium (APWCS)*, 2024, pp. 1–5.

- [108] N. Ginige, A. S. d. Sena, N. H. Mahmood, M. D. Renzo, N. Rajatheva, and M. Latva-Aho, "Nested tensor-based channel estimation for stacked intelligent metasurface-assisted wireless networks," *IEEE Commun. Lett.*, vol. 29, no. 11, pp. 2731–2735, Nov. 2025.
- [109] A. Lawal, A. Zerguine, A. A. Nasir, and K. Abed-Meraim, "Channel estimation for stacked intelligent metasurface-aided network using deep learning," *IEEE Commun. Lett.*, vol. 29, no. 11, pp. 2641–2645, Nov. 2025.
- [110] S. Lin, J. An, L. Gan, M. Debbah, and C. Yuen, "Stacked intelligent metasurface enabled LEO satellite communications relying on statistical CSI," *IEEE Wireless Commun. Lett.*, vol. 13, no. 5, pp. 1295–1299, May 2024.
- [111] E. Shi, J. Zhang, J. An, G. Zhang, Z. Liu, C. Yuen, and B. Ai, "Joint AP-UE association and precoding for SIM-aided cell-free massive MIMO systems," *IEEE Trans. Wireless Commun.*, vol. 24, no. 6, pp. 5352–5367, Jun. 2025.
- [112] H. Niu, J. An, T. Wu, J. Chen, Y. Zhao, Y. L. Guan, M. D. Renzo, M. Debbah, G. K. Karagiannidis, H. Vincent Poor, and C. Yuen, "Introducing meta-fiber into stacked intelligent metasurfaces for MIMO communications: A low-complexity design with only two layers," *IEEE Trans. Wireless Commun.*, pp. 1–16, 2025, Early Access.
- [113] M. Rezvani, R. Adve, A. b. Sediq, and A. El-Keyi, "Uplink wave-domain combiner for stacked intelligent metasurfaces accounting for hardware limitations," in *Proc. IEEE Int. Conf. Commun.*, 2025, pp. 2424–2429.
- [114] M. Nerini and B. Clerckx, "Physically consistent modeling of stacked intelligent metasurfaces implemented with beyond diagonal RIS," *IEEE Communications Letters*, vol. 28, no. 7, pp. 1693–1697, Jul. 2024.
- [115] A. Abrardo, G. Bartoli, and A. Toccafondi, "A novel comprehensive multiport network model for stacked intelligent metasurfaces (SIM) characterization and optimization," *IEEE Trans. Commun.*, vol. 73, no. 11, pp. 11 559–11 573, Nov. 2025.
- [116] N. S. Perović, E. E. Bahngayi, and L.-N. Tran, "Energy-efficient designs for SIM-based broadcast MIMO systems," *IEEE Trans. Commun.*, pp. 1–16, 2025, Early Access.
- [117] E. Shi, J. Zhang, J. An, M. D. Renzo, B. Ai, and C. Yuen, "Energy-efficient SIM-assisted communications: How many layers do we need?" *IEEE Trans. Wireless Commun.*, pp. 1–16, 2025, Early Access.
- [118] X. Gao, Q. Ma, Z. Gu, W. Y. Cui, C. Liu, J. Zhang, and T. J. Cui, "Programmable surface plasmonic neural networks for microwave detection and processing," *Nature Electronics*, vol. 6, no. 4, pp. 319–328, Apr. 2023.